7-1-2020

Phylogeography of the Variable Antshrike (Thamnophilus caerulescens), a South American passerine distributed along multiple environmental gradients

Sergio D. Bolívar-Leguizamón
Universidade de Sao Paulo - USP

Luís F. Silveira
Universidade de Sao Paulo - USP

Elizabeth P. Derryberry
The University of Tennessee, Knoxville

Robb T. Brumfield
Louisiana State University

Gustavo A. Bravo
Universidade de Sao Paulo - USP

Recommended Citation

Bolívar-Leguizamón, S., Silveira, L., Derryberry, E., Brumfield, R., & Bravo, G. (2020). Phylogeography of the Variable Antshrike (Thamnophilus caerulescens), a South American passerine distributed along multiple environmental gradients. *Molecular Phylogenetics and Evolution, 148* https://doi.org/10.1016/j.ympev.2020.106810

Molecular Phylogenetics and Evolution 148 (2020) 106810

Contents lists available at ScienceDirect

Molecular Phylogenetics and Evolution

journal homepage: www.elsevier.com/locate/ympev

Phylogeography of the Variable Antshrike (*Thamnophilus caerulescens*), a South American passerine distributed along multiple environmental gradients

Sergio D. Bolívar-Leguizamón[a,*], Luís F. Silveira[a], Elizabeth P. Derryberry[b], Robb T. Brumfield[c,d], Gustavo A. Bravo[a,e,f]

[a] Museu de Zoologia da Universidade de São Paulo, 04263-000 Ipiranga, São Paulo, SP, Brazil
[b] Department of Ecology and Evolutionary Biology, University of Tennessee, Knoxville, TN 37996, USA
[c] Department of Biological Sciences, Louisiana State University, Baton Rouge, LA 70803, USA
[d] Museum of Natural Science, Louisiana State University, Baton Rouge, LA 70803, USA
[e] Department of Organismic and Evolutionary Biology, Harvard University, Cambridge, MA 02138, USA
[f] Museum of Comparative Zoology, Harvard University, Cambridge, MA 02138, USA

ARTICLE INFO

Keywords:
Circum-Amazonian distribution
Forest Refugia Hypothesis
Demographic modeling
Ultraconserved elements
SNPs
Climatic fluctuations

ABSTRACT

The Neotropics show a wealth of distributional patterns shared by many co-distributed species. A distinctive pattern is the so-called "circum-Amazonian distribution," which is observed in species that do not occur in Amazonia but rather along a belt of forested habitats spanning south and east of Amazonia, the Andean foothills, and often into the Venezuelan Coastal Range and the Tepuis. Although this pattern is widespread across animals and plants, its underlying biogeographic mechanisms remain poorly understood. The Variable Antshrike (*Thamnophilus caerulescens*) is a sexually dimorphic suboscine passerine that exhibits extreme plumage variation and occurs along the southern portion of the circum-Amazonian belt. We describe broad-scale phylogeographic patterns of *T. caerulescens* and assess its demographic history using DNA sequences from the mitochondrion and ultraconserved elements (UCEs). We identified three genomic clusters: a) northern Atlantic Forest; b) south-eastern Cerrado and central-southern Atlantic Forest, and c) Chaco and Andes. Our results were consistent with Pleistocene divergence followed by gene flow, mainly between the latter two clusters. There were no genetic signatures of rapid population expansions or bottlenecks. The population from the northern Atlantic Forest was the most genetically divergent group within the species. The demographic history of *T. caerulescens* was probably affected by series of humid and dry periods throughout the Quaternary that generated subtle population expansions and contractions allowing the intermittent connection of habitats along the circum-Amazonian belt. Recognizing the dynamic history of climate-mediated forest expansions, contractions, and connections during the South American Pleistocene is central toward a mechanistic understanding of circum-Amazonian distributions.

1. Introduction

The Neotropics harbor the highest levels of species diversity and endemism across multiple taxonomic groups (Dinerstein et al., 2017; Halffter, 1992; Mittermeier et al., 1998; Myers et al., 2000; Olson et al., 2001). In general, the geographic distribution of Neotropical organisms results from large-scale geological processes, such as the uplift of the Andes, that generate opportunities for allopatric differentiation and promote diversification into novel environments (Graham, 2009; Hernández-Romero et al., 2017; Herzog et al., 2011; Hooghiemstra et al., 2002; Hoorn et al., 2010; Prieto-Torres et al., 2018). These processes are also shaped by species' dispersal and ecological affinities that affect their ability to move across barriers and persist over time under different environmental conditions (Burney and Brumfield, 2009; Smith et al., 2014), generating a complex mosaic of species distributions often shared by large numbers of co-distributed populations with similar geographic boundaries (Banda et al., 2016; Naka and Brumfield, 2018). Coarse distributional limits of South American taxa have allowed us to recognize the main domains of forested areas, such as the Atlantic Forest and Amazonia, or open areas such as the Llanos and the Cerrado

* Corresponding author.
E-mail addresses: bolivaruis@gmail.com, eldarin2003@yahoo.com (S.D. Bolívar-Leguizamón).

https://doi.org/10.1016/j.ympev.2020.106810
Received 2 October 2019; Received in revised form 23 January 2020; Accepted 25 March 2020
Available online 05 April 2020

(Darlington, Jr., 1957; Morrone, 2014; Sánchez-González et al., 2008). However, prevalent taxon-specific and scale-dependent variation in demographic and geologic histories obfuscate our understanding of the mechanisms driving the evolutionary history of co-existing populations (Smith et al., 2014).

Distributional patterns of Neotropical birds are primarily bounded by the main biogeographic domains (Stotz et al., 1996). However, in numerous instances several widely distributed co-occurring taxa exhibit rather odd distributions that expand beyond the boundaries of these domains. One of these common patterns is known as the circum-Amazonian distribution (*sensu* Remsen et al., 1991), which largely mirrors the extent of Seasonally Dry Tropical Forests – SDTF (*sensu* Mooney et al., 1995) surrounding Amazonia (Chaco, Caatinga, Interandean valleys) but that expands into neighboring forested formations in seasonal savannah environments (Cerrado, Llanos, Pampas) and humid forests (Atlantic Forest, Andean Foothills, Guiana Shield). The circum-Amazonian distribution is shared by a diversity of bird, insect, and plant species (Banda et al., 2016; Bates, 1997; Irmler, 2009; Knapp, 2002; Prado and Gibbs, 1993; Savit and Bates, 2015), but we still lack a thorough understanding of the historical events and evolutionary processes producing this pattern.

Although several hypotheses about the origin and maintenance of diversity in the Neotropics have been proposed for Amazonia (reviewed by Haffer, 1997), they can also be relevant to shed light on the mechanisms underlying circum-Amazonian distributions. For example, the Forest Refugia Hypothesis (Haffer, 1969; Vanzolini and Williams, 1981), which proposes that a series of climatic fluctuations molded the biodiversity in Amazonia during the Cenozoic through cyclic reductions of humid forests, could be extrapolated to explain how a climate-driven dynamic history of isolation during dry periods and secondary contact during humid periods gave rise to distributional patterns along the Andean foothills, the South American Dry Diagonal, and the Atlantic Forest (Carnaval et al., 2009; Prado and Gibbs, 1993; Werneck et al., 2012). More broadly, the secondary contact between populations could generate a continuum of possible outcomes that have speciation and reticulation at its opposite ends (Coyne and Orr, 2004). Presumably, in populations of circum-Amazonian taxa, neither of these processes were complete, leading to the formation of a mosaic of admixed populations with distinct demographic histories. Hence, specific predictions derived from the Forest Refugia Hypothesis pertaining to circum-Amazonian taxa include those of demographic stability in areas of putative refugia, signals of population expansions outside refugia, and noticeable population structure across their entire range. Likewise, the presence of rivers acting as barriers between populations – the Riverine Hypothesis (Capparella, 1988; Sick, 1967; Wallace 1854) – could explain the discontinuous distribution of populations along rivers, such as the São Francisco, the Paraguay, and the Paraná (Fig. 1a). One of the main distinctions between the the Riverine and Forest Refugia Hypotheses is that demographic fluctuations should not be detected under the Riverine Hypothesis, because cycles of extinction and expansion are not expected (Amaral et al., 2013; Maldonado-Coelho, 2012). Also, if these rivers acted as primary barriers for divergence, the location of genetic breaks between populations would match that of rivers instead of those of putative refugia, and estimated divergence times would coincide with the age of rivers.

The Variable Antshrike (*Thamnophilus caerulescens*) is a suboscine passerine that exhibits a partial circum-Amazonian distribution spanning the Atlantic Forest, Cerrado, Chaco, and Andean eastern foothills south of the Marañón Valley (Fig. 1). It inhabits the forest understory, second-growth woodland, and patches of thickets and trees in more open regions, and can use patches of degraded forest remnants (Zimmer and Isler, 2003). *Thamnophilus caerulescens* is sexually dichromatic and exhibits unusually high levels of plumage variation across its range (Marcondes et al., n.d.). Hence, taxonomists have recognized several subspecies (see Zimmer and Isler, 2003) to recognize populations that show stable, diagnosable phenotypic traits across major regions; the general pattern is that of a step cline with the palest populations in the driest areas (Brumfield, 2005; Isler et al., 2005; Marcondes et al., n.d.), conforming to Gloger's Rule (Delhey, 2017; Rensch, 1929). The mechanisms giving rise to such high levels of phenotypic variation without defined geographical boundaries remain poorly understood.

Here, we describe the broad-scale phylogeographic and demographic history of *Thamnophilus caerulescens*. We used sequences of mitochondrial DNA and single nucleotide polymorphisms (SNP) obtained from flanking regions of ultraconserved elements (Bejerano et al., 2004; Faircloth et al., 2012) to a) describe population structure across the range of *T. caerulescens* and to estimate divergence times between populations, and b) assess plausible historical and evolutionary processes associated with the circum-Amazonian distributional pattern of *T. caerulescens*, primarily in light of the Forest Refugia hypothesis. Specifically, we assessed the role of population isolation due to climatic fluctuations in the Cenozoic followed by gene flow between populations during the Quaternary. To this end, we evaluated demographic scenarios that represented different rates and directions of migration and population growth rates. Also, we describe a plausible phylogeographic scenario of the species. The evolutionary and demographic information from populations of *T. caerulescens* is useful in shedding light on the role of lineage-specific histories and idiosyncrasies in shaping circum-Amazonian populations.

2. Materials and methods

2.1. Sampling and DNA extractions

We sampled a total of 53 vouchered specimens of *T. caerulescens*, covering the extent of its geographic distribution (approximately 7 samples/subspecies, min = 1 [*ochraceiventer*], max = 21 [*caerulescens*]; Table S1; Fig. 1) and including all subspecies currently recognized by Zimmer and Isler (2003) and Dickinson and Christidis (2014). Additionally, based on results by Brumfield and Edwards (2007), we sampled three vouchered specimens of the closely related species *T. aethiops*. We extracted total genomic DNA from muscle samples using the PureLink® Genomic DNA Mini kit (Invitrogen Inc) following guidelines by the manufacturer. We quantified genomic DNA concentrations using a Qubit 2.0 fluorometer with the dsDNA BR assay kit (Life Technologies, Inc).

2.2. Mitochondrial DNA

We sequenced the mitochondrial gene *NADH dehydrogenase 2* (ND2) for all individuals of *T. caerulescens* and three individuals of the outgroup. We amplified and sequenced ND2 using standard PCR and Sanger sequencing protocols described elsewhere (Brumfield et al., 2007). We edited sequences and checked that they did not include stop codons or anomalous residues using Geneious v. 11.1.4 (www.geneious.com, Kearse et al., 2012). We aligned sequences with the MAFFT v.7 multiple alignment plugin (Katoh and Standley, 2013) implemented in Geneious. Our final alignment contained 1,041 bp for a total of 55 samples. Newly obtained sequences were deposited in GenBank (Accession numbers MT079216 – MT079269).

To visualize the relationships among mitochondrial haplotypes, we built a Median Joining Network – MJN – haplotype network (Bandelt et al., 1999) implemented in POPART (Leigh and Bryant, 2015). Outgroup samples and short ingroup sequences (< 825 bp) were excluded from the haplotype network and the matrix was trimmed to exclude any positions containing missing data (825 bp, 51 samples). Using the untrimmed alignment (1,041 bp), we estimated genetic diversity (π, θ_W) and Tajima's D to summarize molecular variation and infer possible populational changes. Also, to detect population differentiation we performed an Analysis of molecular Variance (AMOVA) using the packages *pegas* (Paradis, 2010), *adegenet* (Jombart, 2008), and *poppr* (Kamvar et al., 2015, 2014) in R.

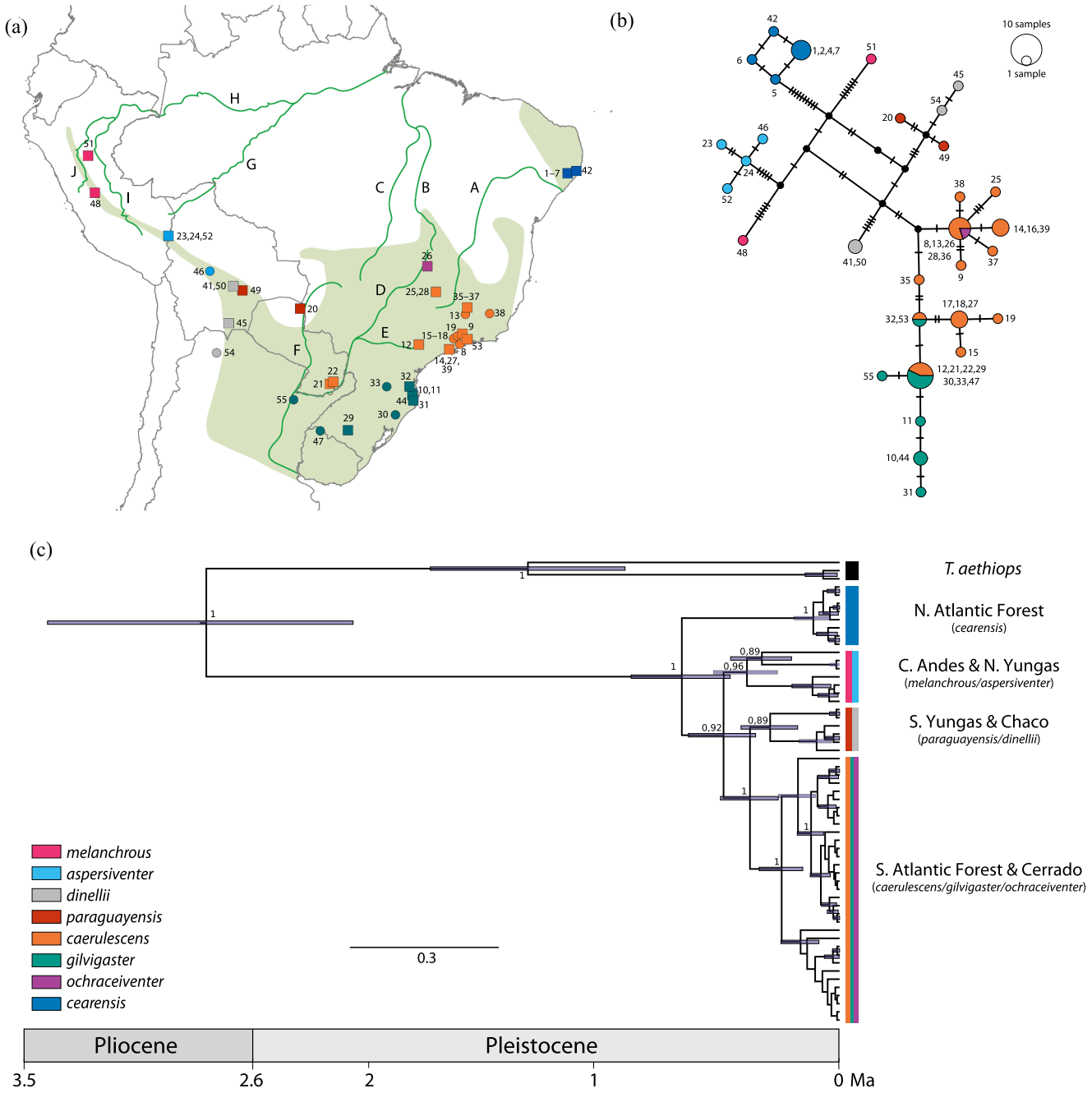

Fig. 1. (a) Locations of sampled specimens of *Thamnophilus caerulescens* (see details in Table S1.) used in this study. Circles represent individuals for which mtDNA (ND2) only was generated, whereas squares denote samples with ND2 and UCE data. Colors represent the eight currently recognized subspecies by Zimmer and Isler (2003). The shaded region represents the extant distribution of the species according to BirdLife International. (b) Median-joining network depicting relationships among the ND2 haplotypes (825 bp). The size of each circle is proportional to the corresponding haplotype frequency. Inferred intermediate haplotypes are shown as black circles on branches connecting observed haplotypes. Tick marks between haplotypes denote additional mutational steps. Colors follow the same scheme as panel 2a. (c) Time-calibrated mtDNA gene tree based on a strict molecular clock with a mtDNA substitution rate corrected by body mass (Nabholz et al., 2016). Colored bars in front of tree represent original subspecies assignments for individuals in each clade. Although differences between subspecies are represented by few mutational steps and some subspecies even share haplotypes, intraspecific mitochondrial variation in *T. caerulescens* is geographically structured. Samples from the northern Atlantic Forest (*cearensis*) are the most divergent and were inferred to have split from the rest around 1.2 Ma ago.

We implemented the corrected Akaike Information Criterion (AICc; Hurvich and Tsai, 1989) in jModeltest2 (Darriba et al., 2012) on the Cipres Science Gateway V 3.3 (Miller et al., 2010) to select the best substitution model (TrN + I + G) on the complete matrix. We estimated a time-calibrated gene tree within a Bayesian framework implemented in the program BEAST2 v2.4.4 (Bouckaert et al., 2014). Based on the method proposed by Nabholz et al. (2016), we used a body mass correction (19.5 g, based on) to estimate a mean substitution rate for ND2 of 0.0187 subst/site/myr. We used a strict molecular clock and a Coalescent Constant Population prior with no restrictions on tree shape and a randomly generated tree as a starting tree. We ran analyses for a total of 50 million generations with a sampling frequency of 1,000. We determined that replicate analyses converged (effective sample size values > 400) using Tracer 1.7.1 (Rambaut et al., 2018). Using TreeAnnotator v2.4.4 (Bouckaert et al., 2014; Drummond et al., 2012) and a burn-in of 30%, we generated a maximum clade credibility (MCC)

with a posterior probability limit of 50%.

2.3. Sequence capture

Based on the results of the mtDNA analyses and aiming at maintaining comprehensive taxonomic and geographical sampling, we followed a target enrichment approach to sequence ultraconserved elements (UCEs; Faircloth et al., 2012) for 28 individuals of *T. caerulescens* and three samples of *T. aethiops*. The genomic enrichment and Illumina sequencing was performed by Rapid Genomics LLC (Gainesville, FL) using at least 1 μg of genomic DNA for each sample. Libraries were enriched from 2,386 UCE loci that targeted a set of 2,560 probes (Faircloth et al., 2012, Tetrapods-UCE-2.5 K version 1; Microarray, Ann Arbor, MI), following an open-source protocol available at www.ultraconserved.org. Samples were multiplexed at 192 samples per lane on a 125 bp paired-end Illumina HiSeq 2500 run (sample pooling was performed at Rapid Genomics with samples from other projects), and the average coverage per *T. caerulescens* sample was 18.6X.

2.4. Edition and assembly of UCEs

We followed the pipeline *Phyluce* v1.6 (Faircloth, 2016, https://github.com/faircloth-lab/phyluce) to process the raw reads and assembly contigs corresponding to target loci. Initially, Illumiprocessor 2.0.7 (Faircloth, 2013) and Trimmomatic 0.32 (Bolger et al., 2014) were used to trim adapters, barcodes, and low quality regions. We used Trinity 2.0.6 (Grabherr et al., 2011) to perform the contig assembly (script *phyluce_assembly_assemblo_trinity*). To avoid including markers of different ploidy, we identified, extracted, and removed Z-linked UCEs from the assemblies using Blast 2.7.7 (see Altschul et al., 1990; Camacho et al., 2009). Z-linked loci were removed from downstream analyses to sample autosomal coalescent histories only and to avoid biases in haplotype calling resulting from differential population sex ratios. Finally, we implemented the script *phyluce_assembly_match_contigs_to_probes* to match the assembled contigs to the UCE probes (uce-2.5 k-probes.fasta). In the end, we recovered 5,702,659 reads in average per sample (N = 28; min = 1,904,001 and max = 10,284,782) after trimming. The assembly produced 17,803 contigs in average per sample (total = 498,503, min = 4,888, max = 143,662) with an average length of 464.53 bp, for a total of 185,331,752 bp. Were recovered a total of 4,697 contigs with more of 1 kb of length, 2,385 of those matching the 2,560 loci in the Tetrapods-UCE-2.5 K probe set.

2.5. Single nucleotide polymorphism (SNP) calling

We extracted Single Nucleotide Polymorphisms (SNPs) from the UCE alignments using the methods described by Harvey et al. (2016), which are largely based on Phyluce (Faircloth, 2016). We extracted SNPs following two approaches that use the function *phyluce_assembly_match_counts*. The first one yielded a 100% complete matrix with no missing data (i.e., no missing SNPs) for any individual in all loci (ingroup individuals = 28, loci = 324), and the second one yielded an incomplete matrix including all data matching the target loci (ingroup individuals = 28, loci = 2,036, 7% of missing SNPs in the matrix). When three individuals of the outgroup were included these matrices contained 201 and 1,954 loci, respectively. The average number of loci per individual was 2,004, and the average number of individuals per locus was 27.

To call SNPs, we first created *fasta files containing the loci extracted from each contig that matched to our target loci (*phyluce_assembly_explode_get_fastas_file*). We chose as a reference the individual with the deepest coverage and longest mean length of recovered contigs (*phyluce_assembly_get_trinity_coverage*, and *phyluce_assembly_get_fasta_lengths*). Then, we used bwa 0.7.7 (Li and Durbin, 2009) to map raw reads from the samples for each group with their respective reference (Li, 2013), and SAMtools 0.1.19 (Li et al., 2009) and Picard (Broad Institute, 2019, http://broadinstitute.github.io/picard/) to create *bam files and mark PCR duplicates. We used GATK 3.8.0 (McKenna et al., 2010) to extract indels, SNPs, and phase sequences. Created *vcf files were exported into other formats for downstream demographic analyses (*nexus, *sfs.gz). Finally, we filtered loci in the complete and incomplete matrices by selecting one random SNP per locus from the biallelic SNPs recovered in each file (script randSnps.pl, https://github.com/caballero/Scripts/). In the end, our datasets contained 324 and 2,036 SNPs in the complete and incomplete matrices, respectively. We implemented all downstream analyses on both matrices to assess potential effects of missing data and matrix size.

2.6. Population structure

To infer population structure from the SNPs, we implemented two multivariate approaches: (1) a Principal Components Analysis (PCA) with the R packages *adegenet/ape* (Jombart, 2008; Paradis et al., 2004); (2) a coefficients of mixture analysis with sparse nonnegative matrix factorization for clustering (sNMF) in the R package *LEA* (Frichot et al., 2014; Frichot and François, 2015) with the following parameters: five α (regularization parameter) values (10, 50, 100, 500, 1000), K values of 1 to 12 (K = 1:12), and 100 runs per K value, and the minimum cross entropy as TRUE to estimate the best number of K. Additionally, we implemented a Discriminant Analysis of Principal Components (DAPC; Jombart et al., 2010) within the *adegenet* package recovering PCs with 80% of variance, and a maximum of 10 groups. Finally, we estimated genetic diversity (π, θ_W), Tajima's D, and performed an Analysis of Molecular Variance (AMOVA) for the incomplete matrix using *pegas* (Paradis, 2010) in R, DNAsp v6.0 (Rozas et al., 2017) and VCFtools (Danecek et al., 2011).

2.7. Species trees

We ran two million iterations in SNAPP with a sampling frequency of 1,000 (Bryant et al., 2012) to identify the relationships among the three distinct clusters (1. northern Atlantic Forest; 2. southeastern Cerrado, central, and southern Atlantic Forest; 3. Chaco and central Andes) recovered in the PCA and sNMF analyses, plus the outgroup *T. aethiops*. We used default values for the backward (u) and forward (v) mutation rates and the value of λ with a gamma distribution (α = 2). We checked that effective sample size values > 400 using Tracer 1.7.1 (Rambaut et al., 2018), and we used Figtree 1.4.4 (Rambaut, 2009) to visualize the results.

2.8. Demographic history

We used the software *momi2* (https://github.com/popgenmethods/momi2; Kamm et al., 2019) to infer possible demographic scenarios in *T. caerulescens*. *Momi2* infers demographic histories by fitting the observed value of the sample frequency spectrum to its expected value in a composite likelihood framework. In this way, multiple demographic models were assessed and the best-fit scenario was selected using the Akaike Information Criterion (AIC, Akaike, 1973). We tested multiple models with different demographic scenarios for the genetic groups identified in the population structure analyses (see details below). Thus, we tested three main types of models (Fig. 2, all models in Fig. S1a-S1b) considering three genetic clusters: 1) northern Atlantic Forest; 2) southeastern Cerrado, central and southern Atlantic Forests; and 3) the Andean and Chacoan populations. The first group of models inferred possible events of migration and divergence times between the three clusters (Fig. 2a). The second group included the parameters of the first group and events of population expansion of the southern Atlantic Forest and Andean clusters, assuming a startpoint of dispersion in the northern Atlantic Forest and posterior expansion to the south (Fig. 2b).

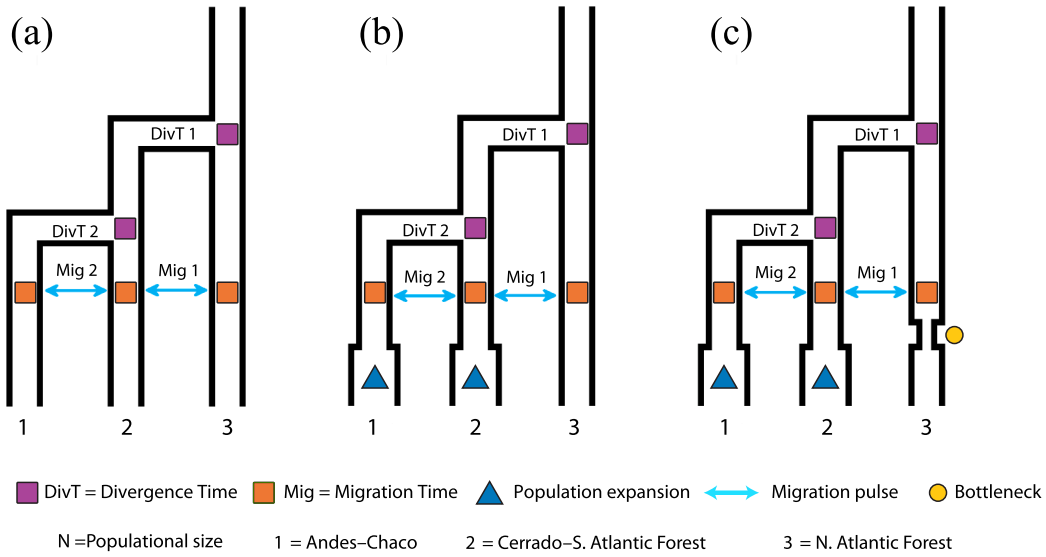

Fig. 2. Schematic of the three groups of demographic models tested in momi2 for the genomic clusters identified for *T. caerulescens* via PCA and DPCA. (a) Models characterizing migration and divergence events only. (b) Models representing expansion events in the Andes-Chaco and Cerrado–S. Atlantic Forest clusters assuming a start point of dispersion in the northern Atlantic Forest and posterior expansion to the south. These models also considered those migration and divergence parameters in the first group of models. (c) Models assuming a bottleneck event in the northern Atlantic Forest after the split from the remaining populations. These models also considered parameters in previous two groups of models.

These additional parameters and assumptions respond to the fact that the northern Atlantic Forest population was consistently recovered as the first split in the species tree analyses (see details below) and that it occurs in an area of putative stability with little forest contraction and expansion and where one of the main Pleistocene refugia in the Atlantic Forest has been proposed (Carnaval et al., 2009; Carnaval and Moritz, 2008). Finally, the third group of models included a bottleneck event in the northern Atlantic Forest after the split from the remaining populations representing the stage of forest contraction preceding a likely refugium scenario (sensu Carnaval et al., 2009; Carnaval and Moritz, 2008; Fig. 2c). For each model, we implemented 100 runs to avoid suboptimal results. Based on the run with the highest likelihood for each model, we evaluated the relative weight of the best model using the Akaike Information Criterion (AIC, Akaike, 1973). We ran 100 bootstrap simulations to estimate confidence intervals of the parameters of the best selected model. We used a mutation rate of 2.5x10^-9 substitutions per site per generation (Nadachowska-Brzyska et al., 2015) and a generation time of 2.33 years, following estimates for other species in the Thamnophilidae (Maldonado-Coelho, 2012; Maldonado-Coelho et al., 2013; Thom et al., 2018).

3. Results

3.1. Mitochondrial divergence and geographic structure

Of the 51 ND2 sequences of *T. caerulescens*, we identified 31 unique haplotypes that were generally structured geographically and that showed considerable numbers of private alleles in the Chaco, Andes, and northern Atlantic Forest (*melanchrous*, *aspersiventer*, *paraguayensis*, *dinellii*, and *cearensis*; Fig. 1). In contrast, we found considerable levels of shared haplotypes among the subspecies occurring in the Cerrado and southern Atlantic Forest (*caerulescens*, *gilvigaster*, and *ochraceiventer*). Bayesian and maximum-likelihood phylogenetic reconstructions showed two strongly supported mitochondrial groups, one in the northern Atlantic Forest and one in the Cerrado and southern–central Atlantic Forest. Moreover, two clades representing populations in the a) southern Yungas and Chaco and b) northern Yungas and the central Andes showed some degree of geographic structure, but their phylogenetic placement was weakly supported and remained unresolved (Fig. 1 & S2). Analyses of divergence times based on the mitochondrial molecular clock estimated that *T. caerulescens* diverged from its closest relatives close to 5 Ma [6.5–3.6 Ma] during the Zanclean period of the early Pliocene. The primary divergence between the population of the northern Atlantic Forest and the other populations took place around 1.2 Ma [1.7–0.8 Ma] during the Calabrian stage of the Pleistocene. The diversification of the remaining clusters occurred during the Middle Pleistocene [0.8–0.3 Ma] (Fig. 1).

3.2. Population structure

Principal component (PCA) and discriminant analyses (DAPC) supported the existence of three genetic clusters within *T. caerulescens* that largely mirrored the mitochondrial results (Fig. 3a). The first group represented the northern Atlantic Forest (subspecies *cearensis*; hereafter '*cearensis* group'). The second group included individuals from the southern–central Atlantic Forest and Cerrado (subspecies *caerulescens*, *gilvigaster*, and *ochraceiventer*; hereafter '*caerulescens* group'). The third group comprised populations from the Chaco, southern and northern Yungas, and central Andes (subspecies *paraguayensis*, *dinelliii*, *aspersiventer*, and *melanchrous*; hereafter '*aspersiventer* group'). We found suggestions of further structure within this last group: an Andean cluster (*melanchrous* and *aspersiventer*) and a Chacoan cluster (*dinelliii* and *paraguayensis*; Fig. S3). Structure in this third group suggested a pattern of continuous or clinal variation running from north to south (*melanchrous – aspersiventer – dinelliii/paraguayensis*; Fig. S4), consistent with previous descriptions of phenotypic and genetic variation in Peru and Bolivia (Brumfield, 2005; Isler et al., 2005). This pattern of differentiation within the *aspersiventer* group was also evident in the subspecific assignments of the DAPC analyses (Tables S4 & S5). Values of the fixation indices (F_{ST}) and analyses of molecular variances (AMOVA) both for the mitochondrial and SNP data supported high population differentiation between these clusters (ND2 [0.23–0.54], SNPs [0.25–0.53]; see details in Tables S6 and S7). Estimates of genetic diversity indicated that the *caerulescens* and *aspersiventer* groups are the most diverse. For all groups, Tajima's D values were negative (ND2 [−3.55 to −0.47], SNPs [−0.70 to −0.30]), consistent with the idea of recent population expansions (see details in Tables S6 and S7).

Structure analyses using sNMF based on the incomplete matrix also

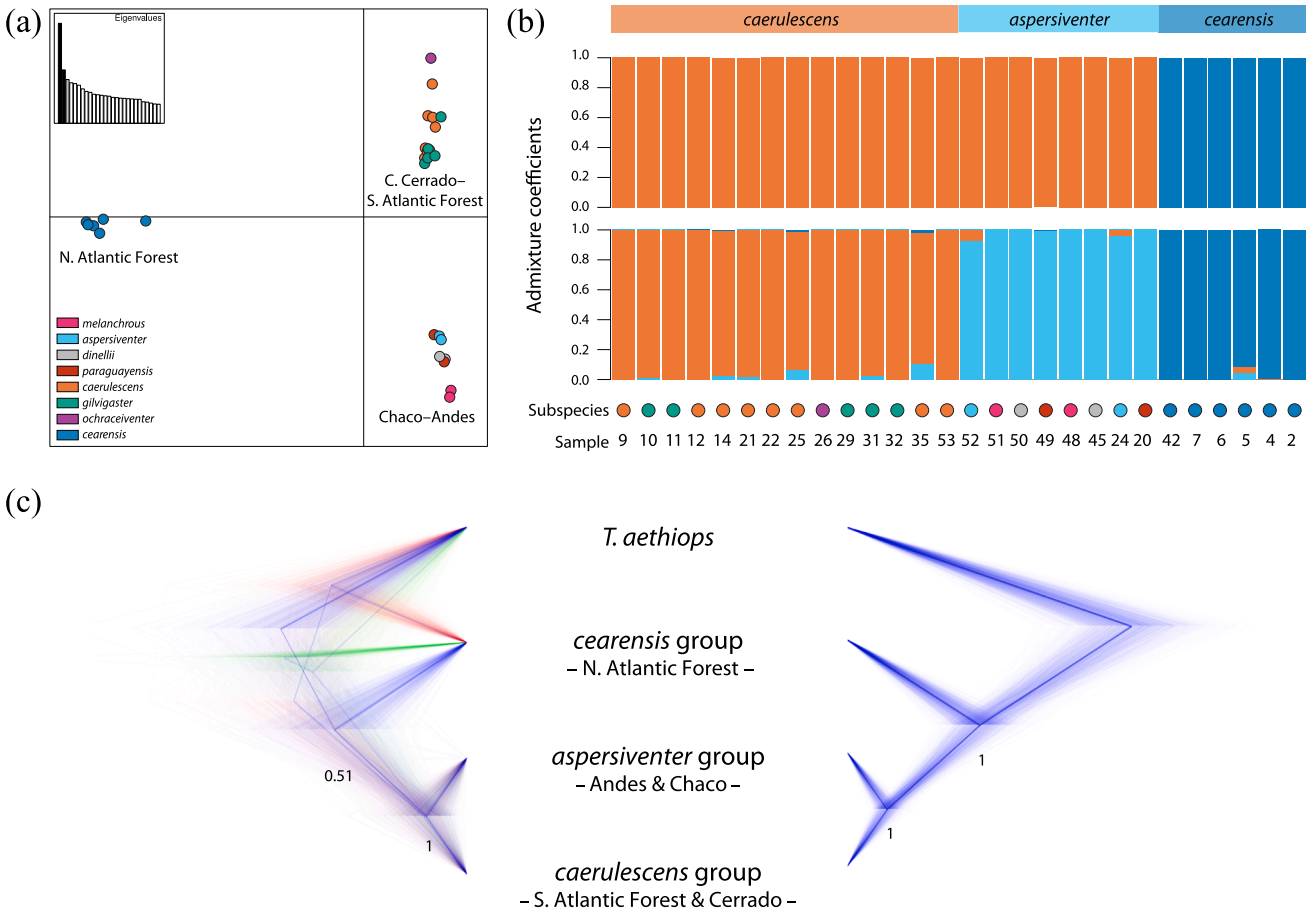

Fig. 3. (a) Principal component analyses based on the incomplete SNP dataset – 2,036 bp. Samples are color-coded by subspecies (b) sNMF population structure of the complete (top; 324 SNPs, K = 2, α = 500, mean cross-entropy = 0.45908) and incomplete (bottom; 2,036 SNPs, K = 3, α = 10, mean cross-entropy = 0.42333) datasets. Each bar represents the admixture coefficients of each individual color-coded by the three genetic clusters identified by PCA and DAPC analyses (top bar). The x-axis shows the subspecies of each individual (colored circles) and its location on the map of Fig. 1 (numbers). (c) Cloudograms of species tree inferences based on the complete (left) and incomplete (right) datasets. Numbers at nodes represent posterior probability values. Results based on the complete matrix favor the existence of two genetic clusters (*cearensis* and *aspersiventer–caerulescens* groups) and the incomplete matrix suggests the existence of three clusters (*cearensis*, *caerulescens*, and *aspersiventer* groups). The *cearensis* group is consistently recovered as the most divergent genetic cluster.

provided support for the three clusters described above (Fig. 3; Table S2). However, the complete matrix supported only two genetic clusters, lumping together the *caerulescens* and *aspersiventer* groups (Fig. 3; Table S3). Surprisingly, sNMF analyses never recovered further structure within the *aspersiventer* group, which is the most heterogeneous of the clusters phenotypically (Brumfield, 2005; Isler et al., 2005; Marcondes et al., n.d.).

3.3. Species tree analyses

Although complete and incomplete matrix analyses yielded similar topological results, suggesting that within *T. caerulescens* the most divergent branch was that of the *cearensis* group, in the former analysis there was no statistical support for the species to be monophyletic (Fig. 3). Specifically, almost half of the inferred species trees in the posterior distribution of the complete matrix analyses placed *cearensis* as sister to the outgroup *T. aethiops*. In contrast, the analyses based on the incomplete matrix showed full support for the *cearensis* group as sister to a clade formed by the *aspersiventer* and *caerulescens* groups.

3.4. Demographic history

The demographic history of *T. caerulescens* was best explained by models considering migration and divergence events only (models 4 & 7 in Fig. S1) that involved asymmetrical gene flow between adjacent populations after initial divergence (Fig. 4; Tables 1 & 2). These uncovered pulses of migration were greater between the *aspersiventer* and *caerulescens* groups, and were considerably lower between the *cearensis* and *caerulescens* groups, suggesting that the level of isolation of the population in the northern Atlantic Forest has been greater than that of the other two groups. Furthermore, these models suggest that the divergence events between populations of *T. caerulescens* occurred during the Middle Pleistocene (0.59–0.81 Ma; Tables S8 & S9).

For the complete matrix, our data were best explained by two largely congruent models that differed in the estimates of initial divergence times and the number of detected migration pulses (Fig. 4; Tables 1 & S8). The most informative model (model 4; log-likelihood = −1,229.45, AIC = 2,476.91 ω_i = 0.62) supported unidirectional migration from north to south (*cearensis* to *caerulescens* to *aspersiventer*) and suggested that those migration pulses occurred after the LGM (*cearensis* to *caerulescens* 19.2 ka [95% CI 16.6–22.2 ka]; *caerulescens* to *aspersiventer* 10.0 ka [95% CI 10.0–10.0 ka]). Additionally, the pulse of migration (here as inferred percentage of N_e that migrated) was greater from the *caerulescens* to the *aspersiventer* group (12.6% [95% CI 11.2–14.0]) than that from the *cearensis* to the *caerulescens* group (3.4% [95% CI 3.2–3.6]). We dated the divergence of the *cearensis* group from the other populations approximately 0.74 Ma (95% CI 0.70–0.78 Ma), whereas the *caerulescens* – *aspersiventer*

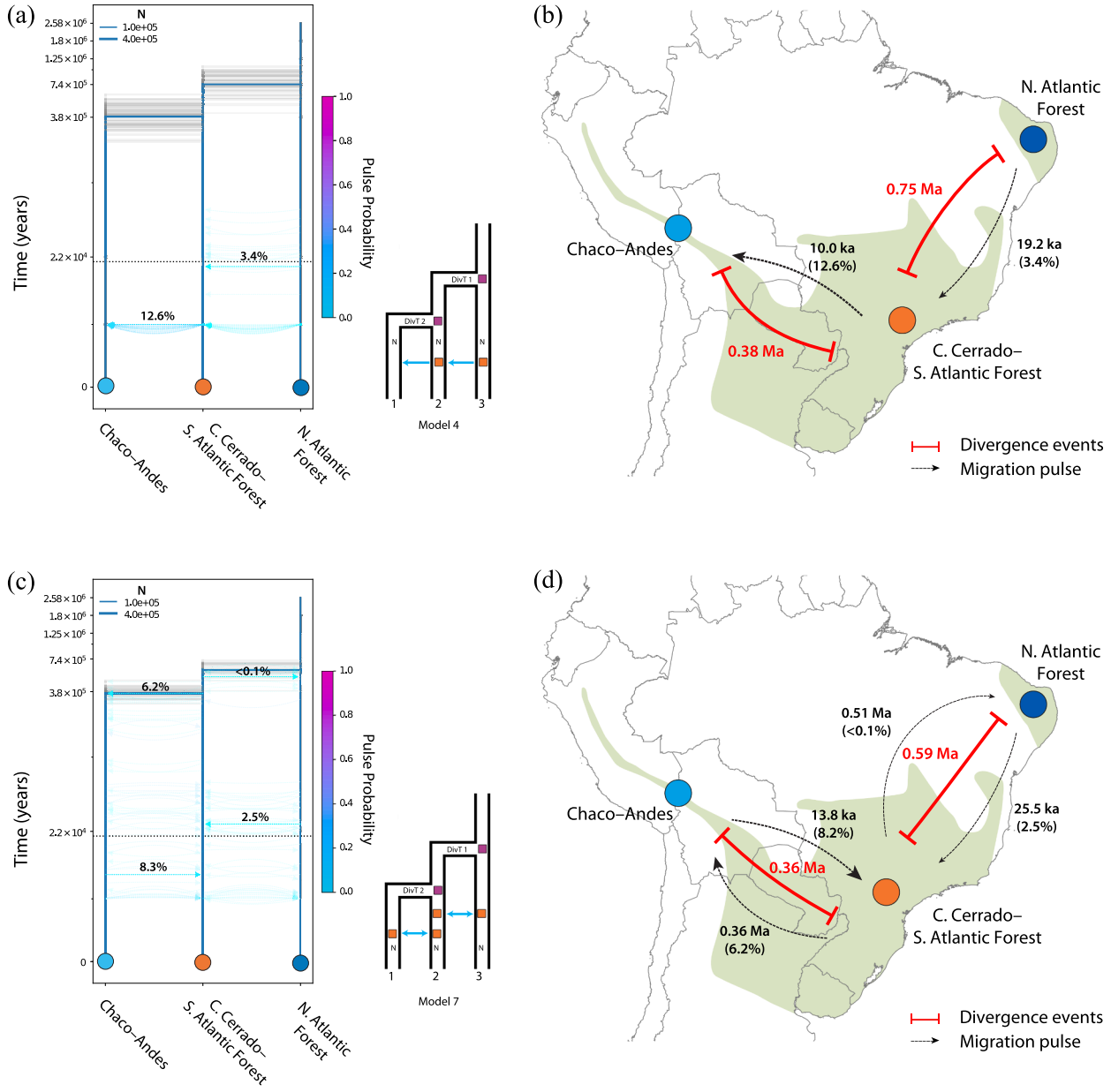

Fig. 4. Temporal (a and c) and geographic (b and d) representations of the most informative demographic models for *Thamnophilus caerulescens* based on the complete (a and b; 324 SNPs) and incomplete matrices (c and d; 2,036 SNPs). The most informative model based on the complete matrix (model 4; log-lik = −1,229.45, AIC = 2,476.91 ω_i = 0.62) depicts a model of unidirectional migrations (a), whereas the one for the incomplete matrix (model 7; log-lik = -7,290.17, AIC = 14,606.33; ω_i = 1) considers bidirectional migrations. In (a) and (c) grey branches represent 100 bootstrap simulations of the model; arrows represent the direction of migration pulses between populations color-coded by migration pulse probability; numbers above arrows of migration pulses also represent migration pulse probability. Small insets represent a cartoon of the model based. In (b) and (d), light blue circle: *aspersiventer* group; Orange circle: *caerulescens* group; Dark blue circle: *cearensis* group. Black dashed arrows: migration pulses. Red solid bars: Divergence times. The shaded region on the map represents the extant distribution of the species according to BirdLife International. No model supported rapid events of population expansion or bottlenecks. Both models support a scenario of Pleistocene diversification of *T. caerulescens* and are concordant with the idea of major gene flow between the *aspersiventer* and *caerulescens* and consider *cearensis* as the most isolated of the clusters. (For interpretation of the references to color in this figure legend, the reader is referred to the web version of this article.)

divergence was traced to 0.38 Ma (95% CI 0.36–0.41 Ma). The second most informative model (model 7; log-lik = -1,225.94, ΔAIC = 0.96 ω_i = 0.38) invoked earlier initial divergence times (0.81 Ma between *cearensis* and the rest; 0.51 Ma between *caerulescens* and *aspersiventer*; Table S8) and supported bidirectional migration pulses between adjacent populations. However, the newly identified pulses of migration were small (4.4% *aspersiventer* to *caerulescens*; < 10E-4% *caerulescens* to *cearensis*; see Table S8 for further details).

For the incomplete matrix, a single model of bidirectional and asymmetrical migration between contiguous populations provided the best fit to our data (model 7; log-lik = −7,290.17, AIC = 14,606.33; ω_i = 1; Fig. 4; Tables 2 & S9). After bootstrapping, we dated the divergence of *cearensis* from the other groups approximately 0.59 Ma (95% CI 0.57–0.61 Ma), whereas the *aspersiventer* – *caerulescens* divergence occurred around 0.36 Ma (95% CI 0.33–0.38 Ma). In this model, events of migration were identified before and after the LGM. The migration from *cearensis* to *caerulescens* occurred about 25.5 ka (95% CI -9.7 to 60.1 ka). The migration from the *caerulescens* to the *aspersiventer* group was estimated 0.36 Ma, and that from *aspersiventer* to *caerulescens* 13.8 ka (95% CI 8.8–18.8 ka). Additionally, the pulses of migrations

Table 1
Information theory statistics and ranking of the 16 demographic models evaluated with momi2 using the complete matrix (324 SNPs). For a complete list of parameter values see Table S8. The most informative models included parameters related to divergence and migration events only.

Rank	Type of model	Model number	Log-lik	Number of parameters	ΔAIC	ω_i
1	**Migrations & divergence**	**4**	**−1229.46**	**9**	0.00	**0.62**
2	**Migrations & divergence**	**7**	**−1225.94**	**13**	0.96	**0.38**
3	Migrations & divergence	6	−1235.11	9	11.31	0.00
4	Migrations & divergence	5	−1240.30	9	21.68	1.21E-05
5	Migrations & divergence	2	−1249.76	4	32.60	5.13E-08
6	Migrations & divergence	3	−1252.65	5	38.38	2.86E-09
7	Migrations, divergence & expansion	10	−1243.96	16	43.00	2.84E-10
8	Migrations & divergence	1	−1258.51	2	44.11	1.63E-10
9	Migrations, divergence & expansion	11	−1247.82	16	50.73	5.94E-12
10	Migrations, divergence & expansion	8	−1252.89	11	50.86	5.56E-12
11	Migrations, divergence, expansion & bottlenecks	13	−1255.51	16	66.10	2.73E-15
12	Migrations, divergence & expansion	9	−1266.95	11	78.98	4.36E-18
13	Migrations, divergence & expansion	12	−1273.97	11	93.03	3.88E-21
14	Migrations, divergence, expansion & bottlenecks	14	−1284.76	11	114.61	8.00E-26
15	Migrations, divergence, expansion & bottlenecks	15	−1294.00	13	132.82	8.90E-30
16	Migrations, divergence, expansion & bottlenecks	16	−1293.87	19	132.82	8.90E-30

Table 2
Information theory statistics and ranking of the 16 demographic model evaluated with momi2 using the incomplete matrix (2,036 SNPs). For a complete list of parameter values see Table S9. The most informative models included parameters related to divergence and migration events only.

Rank	Type of model	Model number	Log-lik	Number of parameters	ΔAIC	ω_i
1	**Migrations & divergence**	**7**	**−7290.17**	**13**	**14606.34**	**1.00**
2	Migrations & divergence	6	−7299.86	9	14617.73	5.32E-10
3	Migrations & divergence	4	−7323.52	9	14665.05	2.83E-20
4	Migrations & divergence	5	−7345.25	9	14708.49	1.04E-29
5	Migrations & divergence	2	−7383.25	4	14776.51	1.77E-44
6	Migrations & divergence	3	−7386.64	5	14783.29	5.96E-46
7	Migrations, divergence & expansion	10	−7388.48	16	14808.97	1.58E-51
8	Migrations, divergence, expansion & bottlenecks	13	−7394.48	16	14820.96	3.93E-54
9	Migrations, divergence & expansion	11	−7394.50	16	14821.00	3.85E-54
10	Migrations & divergence	1	−7481.58	2	14967.16	7.06E-86
11	Migrations, divergence & expansion	12	−7522.21	11	15066.43	1.96E-107
12	Migrations, divergence & expansion	9	−7528.52	11	15079.05	3.57E-110
13	Migrations, divergence & expansion	8	−7574.60	11	15171.20	3.48E-130
14	Migrations, divergence, expansion & bottlenecks	15	−7621.89	13	15281.77	3.40E-154
15	Migrations, divergence, expansion & bottlenecks	16	−7724.95	19	15471.91	1.75E-195
16	Migrations, divergence, expansion & bottlenecks	14	−7807.85	11	15637.71	1.74E-231

were higher when involving both the *caerulescens* and *aspersiventer* groups than when involving the *cearensis* and *caerulescens* groups (see details in Table S9).

4. Discussion

These analyses represent the first comprehensive large-scale phylogeographic study of the Variable Antshrike (*T. caerulescens*) using genomic data. Published analyses aiming at uncovering the evolutionary history of this species focused on few populations, used mitochondrial DNA only (Brumfield, 2005; Isler et al., 2005), or were part of studies at broader phylogenetic scales (Brumfield and Edwards, 2007). Here, we presented results that are congruent across population structure, phylogenetic, and demographic analyses and that provide a good starting point toward the understanding of the demographic history of this species, as well as the mechanisms underlying circum-Amazonian distributions.

4.1. Population structure in Thamnophilus caerulescens

We uncovered the existence of three main genetic clusters within *T. caerulescens*. The first, and most genetically cluster, which we refer to as the *cearensis* group, is composed of samples from the humid Atlantic Forest north of the Rio São Francisco. The second one cluster, which we have denoted the *caerulescens* group, represents the core of the distribution of the species in the southeastern Cerrado and central–southern Atlantic Forest. The third cluster, which we refer to as the *aspersiventer* group, occurs in the transition from those drier environments in the Chaco and southern Yungas in Argentina, Bolivia, and Paraguay to the more humid forests in the northern Yungas and Central Andes in northern Bolivia and Peru. This group covers the region in Bolivia where extreme geographic variation in plumage has been described (Brumfield, 2005; Isler et al., 2005; Marcondes et al., n.d.), and we have provided evidence that there might be further genetic structure within this group.

A unique feature of the distribution of *T. caerulescens* is that in the eastern portion of its range the species is restricted to humid and semi-humid forests, whereas in the southern and western regions it occurs in areas of transition between humid and dry forested habitats. The geographic break between the *cearensis* group and the remaining populations is congruent with those of other animal (e.g., Brown, 1979; Costa et al., 2000; Silva et al., 2004; Tabarelli et al., 2010; Bocalini et al., in review this volume) and plant (Fiaschi and Pirani, 2009; Prance, 1982) populations restricted to the humid forests in the northern Atlantic Forest. This region has been recognized as one of the areas of endemism for birds (Silva et al., 2004; Silveira et al., 2003) and it has been proposed to be a Pleistocene refugium (Carnaval et al., 2009; Carnaval and Moritz, 2008). Several studies have documented that populations therein can be highly divergent from populations in the southern Atlantic Forest (Batalha-Filho et al., 2013; DaSilva et al., 2015; Bocalini et al., in review this volume) and are often considered representatives of the Amazonian rather than Atlantic Forest biota (Maldonado-Coelho

et al., 2013; Melo Santos et al., 2007; Tello et al., 2014; Thom and Aleixo, 2015). Interestingly, in the southern Atlantic Forest the single genetic cluster formed by the *caerulescens* group does not coincide with the well-known prominent pattern of geographic structure associated with areas of endemism (Silva et al., 2004), proposed Pleistocene refugia (Carnaval et al., 2009; Carnaval and Moritz, 2008), or with important rivers, low passes, and mountain ranges (e.g., Batalha-Filho et al., 2019; Batalha-Filho and Miyaki, 2016; Pulido-Santacruz et al., 2016; Amaral et al., 2013; Thomé et al., 2010). This population showed no geographic structure south of the Rio São Francisco, a pattern seldom documented in Atlantic Forest organisms (but see Cabanne et al., 2013; Costa et al., 2017). We acknowledge, however, that our sampling does not include the closest known localities south of the Rio São Francisco in the state of Bahia, and their inclusion in future studies might uncover genetic diversity that we did not sample.

The *aspervinter* group is distributed along a steep environmental humidity gradient from the dry lowland and upland Chaco in southern Bolivia to the humid Yungas and Andean forests of northern Bolivia and Peru. Dry forests corridors in that region have been suggested for other organisms (Linares-Palomino et al., 2011; Quijada-Mascarenãs et al., 2007; Savit and Bates, 2015; Werneck et al., 2012, 2011; Corbett et al., in prep) and are critical to understand the pervasive pattern of connections between the Atlantic Forest and the Andes through the Cerrado and Chaco exhibited by taxa with similar distributions to that of *T. caerulescens* (Batalha-Filho et al., 2013; Cabanne et al., 2019; Prates et al., 2017; Trujillo-Arias et al., 2018, 2017). The most intriguing aspect of the *aspersiventer* group is its step-clinal phenotypic variation along this environmental gradient despite its relatively low levels of genetic variation at putative neutral loci. Phenotypic clines have been described in several Andean birds (Areta and Pearman, 2013; Graves, 1991; Seeholzer and Brumfield, 2018; Van Doren et al., 2018) and other taxa (Premoli, 2003), but their causes remain to be understood. Some of the most likely explanations broadly fall within the realm of local adaptation in response to latitudinal and environmental gradients, geological events, climatic variation during the Pleistocene, secondary contact between isolated populations, and hybridization (Chattopadhyay et al., 2017; Luebert and Weigend, 2014; Miller et al., 2010; Herzog and Kattan, 2011; Miller et al., 2010; Polato et al., 2018). For *T. caerulescens*, more robust genomic and geographic sampling efforts, particularly in Peru and Bolivia, linking natural history, phenotypes, and genotypes will be necessary to provide mechanistic explanations for this cline and uncover the genetic basis of the traits involved (Lamichhaney et al., 2019).

By using two separate datasets of different sizes and dissimilar levels of missing data, we attained a notion of the effects of matrix size and missing data on the ability to detect population structure. In general, we found that in all analyses, particularly in PCA, sNMF, and coalescent species tree inference, both datasets yielded fundamentally concordant results. Namely, the *cearensis* group was the most divergent cluster regardless of dataset size, and the remaining individuals could be treated as only one large population or could even be split into two (i.e., *aspersiventer* and *caerulescens* groups) or three populations (i.e., *melanchrous–aspersiventer, dinellii–paraguayensis*, and *caerulescens* group). It was evident that levels of resolution and statistical power were always higher in the incomplete dataset (2,036 loci) than in the complete one (324 loci), which likely was a consequence of information loss. This observation is in agreement with the idea that stringently reduced matrices due to missing data, such our complete matrix, can suffer from underrepresentation of those informative loci with higher mutation rates, which are the ones containing relevant information to unravel population history and accurately infer species trees in a coalescent framework (Hosner et al., 2016; Huang and Knowles, 2016). In the specific case of the coalescent species tree analyses, it has been suggested that their accuracy improves when more loci are considered, even when minimally informative (Blom et al., 2017; Cloutier et al., 2019; Xi et al., 2015), potentially explaining the lack of resolution of our results based on the complete matrix. Therefore, because those methods mentioned above are tolerant to certain levels of missing data, in our analyses more information was lost when loci with any degree of missing data were removed entirely than when we used the incomplete data set.

4.2. Demographic and biogeographic history of *Thamnophilus caerulescens*

Mitochondrial estimates indicated that population divergence within *T. caerulescens* started during the Pleistocene between 1.7 and 0.8 Ma. These values are older than those inferred in our genome-scale demographic analyses (0.81–0.59 Ma), but a direct comparison between these two analyses is misleading because they are based on extremely discordant amounts of data and reflect different genomic processes (Brito and Edwards, 2009). Mitochondrial data represent the history of a single locus with matrilineal inheritance that is calibrated assuming a clock-like substitution process, whereas our UCE dataset represents thousands of loci that provide a better representation of the heterogeneous demographic and coalescent histories at a genomic scale (Bravo et al., 2019), improving the estimation of demographic parameters (Harvey et al., 2016). Regardless of these conceptual differences, our results are congruent in suggesting that current patterns of population diversity emerged during the Early – Middle Pleistocene. Moreover, they are in line with other estimates of divergence times involving *T. caerulescens*. For example, Thom and Aleixo (2015) estimated that this species diversified along the Late Pliocene – Mid Pleistocene using mitochondrial data, and Brumfield and Edwards (2007) estimated the divergence for the 'montane *caerulescens* clade' (*T. caerulescens*, *T. aethiops*, *T. aroyae*, and *T. unicolor*) between 3.6 and 1.6 Ma, relatively congruent with our results.

Our demographic analyses suggested that the history of *T. caerulescens* is best described by events of divergence and subsequent dispersal between adjacent populations with no drastic changes in population sizes as a consequence of rapid expansions or bottlenecks. Admixture events were found to be more pervasive between the *caerulescens* and *aspersiventer* groups, and those between the *cearensis* and *caerulescens* groups were primarily from the former to the latter (Fig. 3). The underlying explanation of these models is primarily grounded on the climatic heterogeneity of South America during the Quaternary that promoted wet-and-dry cycles that affected forest distribution non-uniformly in space and time (reviewed by Baker et al., 2020). These persisting climatic fluctuations challenge the notion of synchronous and homogeneous cycles that had continental-wide uniform effects on forest distributions (i.e., the traditional Forest Refugia Hypothesis). For instance, Cruz et al. (2009) and Wang et al. (2017) described a precipitation dipole from west to east along the equator that varied at orbital time scales (~20 ka) generating reversed cycles of humid and dry habitats in western and eastern tropical South America. Furthermore, short-term (millennial) extreme precipitation and glacial run-off events (Nace et al., 2014; Wang et al., 2017) were common occurrences during the South American glacial cycles of the Pleistocene creating opportunities for finer-scale events of forest connections and disconnections (reviewed by Baker et al., 2020). Possibly the main effects of such cycles and extreme climatic Pleistocene events on populations restricted to forested habitats were asynchronous divergence and admixture events across their range. Therefore, in a widespread species, such as *T. caerulescens*, it is expected that populations did not become isolated or connected simultaneously, as supported by our demographic analyses. Furthermore, such dynamic history makes it difficult, if not impossible, to pinpoint with high confidence individual admixture events at specific points in time because the signature of many admixture events on demographic reconstructions can be noisy (Fig. 4c).

Despite its simplicity relative to the convoluted climatic history of South America during the Pleistocene, the Forest Refugia Hypothesis (Haffer, 1969; Vanzolini and Williams, 1970) and its complementary proposals are still relevant to partially explain the demographic history

of *T. caerulescens*, as they have been for many other taxa (see Campagna et al., 2012; Carnaval and Moritz, 2008; de Oliveira Miranda et al., 2019; García-Vázquez et al., 2017; Leal et al., 2018; Pérez-Escobar et al., 2017; Ramos et al., 2018; Richardson et al., 2001; Thomaz et al., 2015). Although none of the demographic models allowing rapid changes of population sizes were supported in our analyses, basic measurements of genetic diversity of all populations showed signals of recent population expansion (Tables S6 & S7). This observation suggests that the three genetic clusters had smaller population sizes and that their present-time distributions are wider than they were in the past. In the specific case of the *cearensis* group, its allopatric distribution and high levels of differentiation with respect to the other groups are likely consequences of the Pliocene-Pleistocene refugium in north-eastern Brazil (i.e., Pernambuco refugium, *sensu* Carnaval et al., 2009; Carnaval and Moritz, 2008). The extant distribution of the *caerulescens* and *aspersiventer* groups do not coincide fully with the proposed distribution of Pleistocene refugia. However, it is conceivable that during recent forest contraction periods their populations were restricted to refugia-like forest fragments and that recent expansion events generated their present-time distributions. Our estimates of ancestry coefficients and migration rates between the *caerulescens* and *aspersiventer* groups suggest recent admixture between these populations. It is plausible that, after a period of expansion (late Miocene – early Pleistocene, see Prates et al., 2017), a single population comprising these two groups began to separate during the Quaternary but the daughter populations were still subject to secondary contact along an Atlantic Forest – Cerrado – Chaco corridor, leading to the presently observed phenotypic and genetic clines in Bolivia and Peru, where environmental variation is most significant (Brumfield, 2005; Isler et al., 2005).

Pleistocene connections between the Atlantic Forest and the Andes through the Chaco have been proposed. For instance, Batalha-Filho et al. (2013) invoked a plausible connection between species in the genus *Synallaxis* from the central-south Atlantic Forest and the Andes during the Pleistocene. Also, Trujillo-Arias et al., 2018, 2017) found that there might have been connections between the Atlantic Forest and the central Andes during the Pleistocene, conceivably through the Cerrado and, to a lesser extent, the Chaco (see Cabanne et al., 2019). Florentín et al. (2018) suggested that the existence of connections between areas of dry forests from eastern Brazil and the Chaco were an important force in the diversification of the plant genus *Galianthe*.

The existence of these dry forest corridors is partially consistent with the Pleistocene Arch Hypothesis (PAH, Mogni et al., 2015; Prado and Gibbs, 1993). The PAH proposes that relatively stable areas of non-Amazonian forests (mainly Seasonally Dry Tropical Forests – SDTFs) were connected during the humid cycles of the Pleistocene forming a forested corridor running from the Caatinga to the central Andes, thereby allowing gene flow and population expansions. Under this scenario, *T. caerulescens* could have used such corridors to connect those populations in the central-southern Atlantic Forest with those in the Chaco, dry Yungas, and the Central Andes. Because populations in the northern Atlantic Forest are restricted to humid forests, the PAH presumably did not have an effect connecting them with populations in the south, which is consistent with the older divergence time and weaker signatures of migrations observed in the *cearensis* group. Werneck et al. (2011) rejected the idea of a stable PAH connecting patches of SDTF in those areas known today as the Caatinga, Cerrado, and Chaco, and proposed an alternative scenario in which such an arch might have existed earlier, either during the Early Pleistocene or the Tertiary, followed by cycles of fragmentation and secondary expansion during the Holocene. Although our results cannot answer as to whether such forested corridor was present during the Lower Pleistocene or the late Tertiary, they are consistent with the idea of a once continuous population that underwent divergence and subsequent secondary contact during the Pleistocene.

Although the Rio São Francisco and the Rios Paraná and Paraguay (Riverine Hypothesis; Capparella, 1988; Sick, 1967; Wallace, 1854) could potentially explain the divergence between the *cearensis* and *caerulescens* groups and between the *caerulescens* and *aspersiventer* groups, respectively, data from other taxa do not support this hypothesis. For instance, Carvalho et al. (2017) and Maldonado-Coelho et al. (2013) showed that the Rio São Francisco is not an efficient primary barrier to generate population divergence in the northern and central Atlantic Forest. Instead, climatic fluctuations created 'bioclimatic units' based on altitudinal gradients that have a more significant impact on these regions (Carnaval and Moritz, 2008). The Rio São Francisco has been suggested to act as secondary barrier for gene flow between the northern and the central/southern Atlantic Forest populations (D'horta et al., 2011; Werneck et al., 2012), but our estimates of divergence times and the fact that *T. caerulescens* populations are not immediately adjacent to the river channel suggest otherwise. Similarly, although their role as primary barriers has not been widely tested for vertebrates, there is no evidence that the Rios Paraná and Paraguay are primary barriers for divergence (Cáceres, 2007; Kopuchian et al., 2020). Our sampling is not robust enough to thoroughly test this idea for *T. caerulescens*. However, given the known distributional ranges of *T. caerulescens gilvigaster* and *T. c. dinelliii* (Zimmer and Isler, 2003), it is likely that the Rio Paraná also acts as a secondary barrier, particularly along the lower stretch of the river south of Misiones, Argentina. In fact, recent thorough sampling along the lower Rio Paraná suggested that this river plays an important role in maintaining the divergence between the *caerulescens* and *aspersiventer* groups (Kopuchian et al., 2020).

4.3. A likely scenario for the biogeographic history of T. caerulescens

The results of our analyses suggest that the history of *T. caerulescens* began in the Late Miocene-Pliocene, with an initial widespread population distributed across the Cerrado, Atlantic Forests, the Chaco and the central Andes (Fig. 4). During the Early – Middle Pleistocene (0.81–0.59 Ma), climatic fluctuations promoted expansions and contractions of forested habitats separating populations in the northern Atlantic Forest from those farther south. During the Middle Pleistocene (0.50–0.36 Ma), the continued effects of wet-dry cycles caused the contraction of populations in the southern Atlantic Forest and in the Chaco-Andes, but at the same time allowed sufficient opportunities to maintain gene flow via the onset of dry-forest corridors that connected these two regions. Although birds in the northern Atlantic Forest have remained mostly isolated since their initial divergence, it is likely that they have experienced periods of gene flow with populations in the southern Atlantic Forest.

Brumfield and Edwards (2007) placed the origin of *T. caerulescens* in the 'lowlands of eastern Brazil.' If this were the case, then the origin of the entire *aspersiventer* group would be a colonization event from the *caerulescens* group. One of our most informative demographic models supported the idea of migration from the latter to the former as they diverged (Fig. 4c). However, our data lack the power to discern unambiguously between a vicariant and a colonization origin of this population. Likewise, our sampling is not robust enough to unravel the demographic dynamics along the area connecting the Andes and the Chaco, but two plausible scenarios can potentially explain the population structure that we observed within the *aspersiventer* group and its well-known dramatic phenotypic variation. The first one corresponds to the colonization of the Andean forests from populations in the Chaco that rapidly became adapted to the steep environmental gradient therein giving rise to the complex clinal arrangement of phenotypes observed today. The second one invokes secondary contact between two recently diverged and locally-adapted allopatric populations, one in the Andes and one in the Chaco lowlands, that came into contact recently giving rise to a hybrid zone where phenotypic variation conforms to a clinal pattern (Brumfield 2005). Nonetheless, the prevalence of cycles of retractions and expansions of their habitat during the Pleistocene-Holocene were likely critical to generate present-time patterns of population and phenotypic structure in the Chaco–Andes

populations.

5. Conclusions

The Variable Antshrike, *Thamnophilus caerulescens*, is a widespread suboscine passerine with a nearly continuous circum-Amazonian distribution spanning humid and dry forests along the Atlantic Forest, the southern portion of the Cerrado, the Chaco, the southern and northern Yungas and the central Andes. We uncovered the existence of three genetic clusters, one in the northern Atlantic Forest, one in the Cerrado and southern–central Atlantic Forests, and another one in the Chaco–Andes. The first cluster is the most divergent group having split from the rest during the Early – Middle Pleistocene (0.81–0.59 Ma) followed by a split between the two remaining populations during the Mid Pleistocene (0.50–0.36 Ma). Demographic histories of these populations are consistent with a scenario of divergence and subsequent gene flow mediated by climatic fluctuations during the Quaternary. The signature of these dynamic climates on the demographic history of *T. caerulescens* offer partial support for the Forest Refugia Hypothesis. Climate-driven contractions and expansion of forested habitats were certainly responsible for creating refugia-like strongholds of the distribution of the species, particularly in the northern Atlantic Forest. However, these climate-induced habitat shifts likely occurred in asynchronous fashion and had different impacts across the species' range, conflicting with the traditional view of continental-scale cycles affecting communities uniformly. Our data do not support a history of population size changes produced by rapid geographic expansions or population bottlenecks, but rather changes in population sizes were subtle and likely followed the pace of climate-driven habitat shifts.

CRediT authorship contribution statement

Sergio D. Bolívar-Leguizamón: Conceptualization, Methodology, Software, Formal analysis, Investigation, Data curation, Writing - original draft, Writing - review & editing. **Luís F. Silveira:** Funding acquisition, Resources, Supervision, Writing - review & editing. **Elizabeth P. Derryberry:** Funding acquisition, Writing - review & editing. **Robb T. Brumfield:** Conceptualization, Resources, Funding acquisition, Writing - review & editing. **Gustavo A. Bravo:** Conceptualization, Funding acquisition, Resources, Formal analysis, Investigation, Supervision, Methodology, Visualization, Writing - review & editing.

Acknowledgments

We are grateful to the curators and staff of the following institutions for granting us access to tissues under their care: MZUSP – Museu de Zoologia da Universidade de São Paulo; LSUMZ – Louisiana State University Museum of Natural Science; MCP – Coleção de Ornitologia do Museu de Ciências e Tecnologia da Pontifícia Universidade Católica do Rio Grande do Sul; CUMV – Cornell University Museum of Vertebrates; FMNH – Field Museum of Natural History; KU – University of Kansas Natural History Museum; MPEG – Museu Paraense Emílio Goeldi; UWBM – University of Washington Burke Museum. We also thank those field ornithologists who collected the specimens used in the study. We are indebted to M. Lima and M. Félix for their assistance with specimen preparation at the Museu de Zoologia da Universidade de São Paulo – MZUSP. We are particularly grateful to F. Bocalini, J. Battilana, A. M. Cuervo, S. Herke at the Louisiana State University Genomics Facility, and the staff at RAPiD Genomics for assistance with molecular lab work. We thank G. Del-Rio for her guidance with data analyses and G. Derryberry for his assistance with data processing. J. V. Remsen Jr. and two anonymous reviewers provided useful comments that improved the manuscript. Access to the HPC–MZUSP cluster was kindly allowed by T. Grant and H. Zaher, and D. Machado provided support with its use.

Funding

Financial support was provided by the São Paulo Research Foundation – FAPESP (2015/16092-7 to SDB–L; 2012-23852-0 to GAB; 2017/23548-2 to LFS), National Science Foundation – NSF (DEB-1011435 to GAB and RTB; DEB-1146265 to RTB; DEB-1146423 to EPD), and Brazilian Research Council – CNPq (457974-2014-1 to GAB and LFS; 302291/2015-6 to LFS). SDB-L acknowledges financial support from the Coordination for the Improvement of Higher Education Personnel – CAPES and the Frank M. Chapman Memorial Fund from the American Museum of Natural History – AMNH (2016). GAB is gratefult to S. V. Edwards and the Department of Organismic and Evolutionary Biology at Harvard University for providing financial support.

Data accessibility

Data statement: UCE raw read data are available on NCBI SRA 14569426-14569453 (BioProject PRJNA624148). VCF files and ND2 and UCE sequence alignmentsare available on https://github.com/SergioB1983/Tcaerulescens.

Appendix A. Supplementary material

Supplementary data to this article can be found online at https://doi.org/10.1016/j.ympev.2020.106810.

References

Akaike, H., 1973. Information theory and an extension of the maximum likelihood principle. Int. Symp. Inf. theory Inf. an Ext. Theory 267–281.

Altschul, S.F., Gish, W., Miller, W., Myers, E.W., Lipman, D.J., 1990. Basic local alignment search tool. J. Mol. Biol. 215, 403–410. https://doi.org/10.1016/S0022-2836(05)80360-2.

Amaral, F.R. Do, Albers, P.K., Edwards, S.V., Miyaki, C.Y., 2013. Multilocus tests of Pleistocene refugia and ancient divergence in a pair of Atlantic Forest antbirds (*Myrmeciza*). Mol. Ecol. 22, 3996–4013. https://doi.org/10.1111/mec.12361.

Areta, J.I., Pearman, M., 2013. Species Limits and Clinal Variation in a Widespread High Andean Furnariid: The Buff-Breasted Earthcreeper (*Upucerthia validirostris*). Condor 115, 131–142. https://doi.org/10.1525/cond.2012.120039.

Baker, P.A., Fritz, S.C., Battisti, D.S., Dick, C.W., Vargas, O.M., Asner, G.P., Martin, R.E., Wheatley, A., Prates, I., 2020. Beyond Refugia: New Insights on Quaternary Climate Variation and the Evolution of Biotic Diversity in Tropical South America. In: Rull, V., Carnaval, A.C. (Eds.), Neotropical Diversification: Patterns and Processes. Fascinating Life Sciences. Springer, Cham, pp. 51–70. https://link.springer.com/chapter/10.1007/978-3-030-31167-4_3.

Banda, K.R., Delgado-Salinas, A., Dexter, K.G., Linares-Palomino, R., Oliveira-Filho, A., Prado, D., Pullan, M., Quintana, C., Riina, R., Rodríguez, G.M., Weintritt, J., Acevedo-Rodríguez, P., Adarve, J., Álvarez, E., Aranguren, A.B., Arteaga, J.C., Aymard, G., Castaño, A., Ceballos-Mago, N., Cogollo, Á., Cuadros, H., Delgado, F., Devia, W., Dueñas, H., Fajardo, L., Fernández, Á., Fernández, M.Á., Franklin, J., Freid, E.H., Galetti, L.A., Gonto, R., González, R.M., Graveson, R., Helmer, E.H., Idárraga, Á., López, R., Marcano-Vega, H., Martínez, O.G., Maturo, H.M., McDonald, M., McLaren, K., Melo, O., Mijares, F., Mogni, V., Molina, D., Morenodel, N.P., Nassar, J.M., Neves, D.M., Oakley, L.J., Oatham, M., Olvera-Luna, A.R., Pezzini, F.F., Dominguez, O.J.R., Ríos, M.E., Rivera, O., Rodríguez, N., Rojas, A., Särkinen, T., Sánchez, R., Smith, M., Vargas, C., Villanueva, B., Pennington, R.T., 2016. Plant diversity patterns in neotropical dry forests and their conservation implications. Science 353 (80), 1383–1387. https://doi.org/10.1126/science.aaf5080.

Bandelt, H.-J., Forster, P., Röhl, A., 1999. Median-joining networks for inferring intraspecific phylogenies. Mol. Biol. Evol. 16, 37–48.

Batalha-Filho, H., Irestedt, M., Ericson, J.F.P.G.P., Silveira, L.F., Miyaki, C.Y., 2013. Molecular systematics and evolution of the *Synallaxis ruficapilla* complex (Aves: Furnariidae) in the Atlantic Forest. Mol. Phylogenet. Evol. 67, 86–94. https://doi.org/10.1016/j.ympev.2013.01.007.

Batalha-Filho, H., Maldonado-Coelho, M., Miyaki, C.Y., 2019. Historical climate changes and hybridization shaped the evolution of Atlantic Forest spinetails (Aves: Furnariidae). Heredity (Edinb) 123 (5), 675–693. https://doi.org/10.1038/s41437-019-0234-y.

Batalha-Filho, H., Miyaki, C.Y., 2016. Late Pleistocene divergence and postglacial expansion in the Brazilian Atlantic Forest: multilocus phylogeography of *Rhopias gularis* (Aves: Passeriformes). J. Zool. Syst. Evol. Res. 54, 137–147. https://doi.org/10.1111/jzs.12118.

Bates, J.M., 1997. Distribution and geographic variation in three South American grass-quits (Emberizinae, *Tiaris*). Ornithol. Monogr. 48, 91–110.

Bejerano, G., Pheasant, M., Makunin, I., Stephen, S., Kent, W.J., Mattick, J.S., Haussler, D., 2004. Ultraconserved elements in the human genome. Science (80-.) 304, 1321–1325. https://doi.org/10.1126/science.1098119.

Blom, M.P.K., Bragg, J.G., Potter, S., Moritz, C., 2017. Accounting for uncertainty in gene tree estimation: Summary-coalescent species tree inference in a challenging radiation of Australian lizards. Syst. Biol. 66, 352–366. https://doi.org/10.1093/sysbio/syw089.

Bolger, A.M., Lohse, M., Usadel, B., 2014. Trimmomatic: A flexible trimmer for illumina sequence data. Bioinformatics. Bioinfor 30, 2114–2120. https://doi.org/10.1093/bioinformatics/btu170.

Bouckaert, R., Heled, J., Kühnert, D., Vaughan, T., Wu, C.-H., Xie, D., Suchard, M.A., Rambaut, A., Drummond, A.J., 2014. BEAST 2: A software platform for bayesian evolutionary analysis. PLOS Comput. Biol. 10, 1–6. https://doi.org/10.1371/journal.pcbi.1003537.

Bravo, G.A., Antonelli, A., Bacon, C.D., Bartoszek, K., Blom, M.P.K., Huynh, S., Jones, G., Lacey Knowles, L., Lamichhaney, S., Marcussen, T., Morlon, H., Nakhleh, L.K., Oxelman, B., Pfeil, B., Schliep, A., Wahlberg, N., Werneck, F.P., Wiedenhoeft, J., Willows-Munro, S., Edwards, S.V., 2019. Embracing heterogeneity: Coalescing the tree of life and the future of phylogenomics. PeerJ 2019, 1–60. https://doi.org/10.7717/peerj.6399.

Brito, P.H., Edwards, S.V., 2009. Multilocus phylogeography and phylogenetics using sequence-based markers. Genetica 135, 439–455. https://doi.org/10.1007/s10709-008-9293-3.

Broad Institute, 2019. Picard Tools (Accessed: 2018/09/21; version 2.17.8). Broad Institute, GitHub Repos.

Brown, K.S., 1979. Ecologia Geográfica e Evolução nas Florestas Neotropicais. Universidade Estadual de Campinas.

Brumfield, R.T., 2005. Mitochondrial variation in bolivian populations of the variable antshrike (*Thamnophilus Caerulescens*). Auk 122, 414–432. https://doi.org/10.1642/0004-8038(2005)122[0414:MVIBPO]2.0.CO;2.

Brumfield, R.T., Edwards, S.V., 2007. Evolution into and out of the Andes: A bayesian analysis of historical diversification in *Thamnophilus*. Antshrikes. Evolution (N. Y). 61, 346–367. https://doi.org/10.1111/j.1558-5646.2007.00039.x.

Brumfield, R.T., Tello, J.G., Cheviron, Z.A., Carling, M.D., Crochet, N., Rosenberg, K.V., 2007. Phylogenetic conservatism and antiquity of a tropical specialization: Army-ant-following in the typical antbirds (Thamnophilidae). Mol. Phylogenet. Evol. 45, 1–13. https://doi.org/10.1016/j.ympev.2007.07.019.

Bryant, D., Bouckaert, R., Felsenstein, J., Rosenberg, N.A., RoyChoudhury, A., 2012. Inferring species trees directly from biallelic genetic markers: bypassing gene trees in a full coalescent analysis. Mol. Biol. Evol. 29, 1917–1932. https://doi.org/10.1093/molbev/mss086.

Burney, C., Brumfield, R., 2009. Ecology predicts levels of genetic differentiation in neotropical birds. Am. Nat. 174, 358–368. https://doi.org/10.1086/603613.

Cabanne, G.S., Campagna, L., Trujillo-Arias, N., Naoki, K., Gómez, I., Miyaki, C.Y., Santos, F.R., Dantas, G.P.M., Aleixo, A., Claramunt, S., Rocha, A., Caparroz, R., Lovette, I.J., Tubaro, P.L., 2019. Phylogeographic variation within the Buff-browed Foliage-gleaner (Aves: Furnariidae: *Syndactyla rufosuperciliata*) supports an Andean-Atlantic forests connection via the Cerrado. Mol. Phylogenet. Evol. 133, 198–213. https://doi.org/10.1016/j.ympev.2019.01.011.

Cabanne, G.S., Sari, E.H.R., Meyer, D., Santos, F.R., Miyaki, C.Y., 2013. Matrilineal evidence for demographic expansion, low diversity and lack of phylogeographic structure in the Atlantic forest endemic Greenish Schiffornis *Schiffornis virescens* (Aves: Tityridae). J. Ornithol. 154, 371–384. https://doi.org/10.1007/s10336-012-0901-8.

Cáceres, N., 2007. Semideciduous Atlantic Forest mammals and the role of the Paraná River as a riverine barrier. Neotrop. Biol. Conserv. 2, 84–89. https://doi.org/10.4013/5930.

Camacho, C., Coulouris, G., Avagyan, V., Ma, N., Papadopoulos, J., Bealer, K., Madden, T.L., 2009. BLAST+: architecture and applications. BMC Bioinf. 10, 421. https://doi.org/10.1186/1471-2105-10-421.

Campagna, L., Benites, P., Lougheed, S.C., Lijtmaer, D.A., Giacomo, A.S. Di, Eaton, M.D., Tubaro, P.L., 2012. Rapid phenotypic evolution during incipient speciation in a continental avian radiation. Proc. R. Soc. London B Biol. Sci. 279, 1847–1856. https://doi.org/10.1098/rspb.2011.2170.

Capparella, A., 1988. Genetic variation in Neotropical birds: implication for the speciation process. Acta XIX Congr. Intern. Ornith. 2, 1658–1664.

Carnaval, A.C., Hickerson, M.J., Haddad, C.F.B., Rodrigues, M.T., Moritz, C., 2009. Stability predicts genetic diversity in The Brazilian atlantic forest hotspot. Science (80-.) 323, 785–789. https://doi.org/10.1126/science.1166955.

Carnaval, A.C., Moritz, C., 2008. Historical climate modelling predicts patterns of current biodiversity in the Brazilian Atlantic forest. J. Biogeogr. 35, 1187–1201. https://doi.org/10.1111/j.1365-2699.2007.01870.x.

Carvalho, C.D.S., Do Nascimento, N.F.F., De Araujo, H.F.P., 2017. Bird distributional patterns support biogeographical histories and are associated with bioclimatic units in the Atlantic Forest, Brazil. Zootaxa 4337, 223–242. https://doi.org/10.11646/zootaxa.4337.2.3.

Chattopadhyay, B., Garg, K.M., Gwee, C.Y., Edwards, S.V., Rheindt, F.E., 2017. Gene flow during glacial habitat shifts facilitates character displacement in a Neotropical flycatcher radiation. BMC Evol. Biol. 17, 210. https://doi.org/10.1186/s12862-017-1047-3.

Cloutier, A., Sackton, T.B., Grayson, P., Clamp, M., Baker, A.J., Edwards, S.V., 2019. Whole-genome analyses resolve the phylogeny of flightless birds (palaeognathae) in the presence of an empirical anomaly zone. Syst. Biol. 68 (6), 937–955. https://doi.org/10.1093/sysbio/syz019.

Costa, L.P., Leite, Y.L.R., Fonseca, G.A.B., Fonseca, M.T., 2000. Biogeography of South American forest mammals: endemism and diversity in the atlantic forest1. Biotropica 32, 872–881. https://doi.org/10.1111/j.1744-7429.2000.tb00625.x.

Costa, P.C., Lorenz-Lemke, A.P., Furini, P.R., Honorio Coronado, E.N., Kjellberg, F., Pereira, R.A.S., 2017. The phylogeography of two disjunct Neotropical *Ficus* (Moraceae) species reveals contrasted histories between the Amazon and the Atlantic Forests. Bot. J. Linn. Soc. 185, 272–289. https://doi.org/10.1093/botlinnean/box056.

Coyne, J.A., Orr, H.A., 2004. Speciation. Sinauer.

Cruz, F.W., Vuille, M., Burns, S.J., Wang, X., Cheng, H., Werner, M., Lawrence Edwards, R., Karmann, I., Auler, A.S., Nguyen, H., 2009. Orbitally driven east–west antiphasing of South American precipitation. Nat. Geosci. 2, 210–214. https://doi.org/10.1038/ngeo444.

D'horta, F.M., Cabanne, G.S., Meyer, D., Miyaki, C.Y., 2011. The genetic effects of Late Quaternary climatic changes over a tropical latitudinal gradient: diversification of an Atlantic Forest passerine. Mol. Ecol. 20, 1923–1935. https://doi.org/10.1111/j.1365-294X.2011.05063.x.

Danecek, P., Auton, A., Abecasis, G., Albers, C.A., Banks, E., DePristo, M.A., Handsaker, R.E., Lunter, G., Marth, G.T., Sherry, S.T., McVean, G., Durbin, R., 2011. The variant call format and VCFtools. Bioinformatics 27, 2156–2158. https://doi.org/10.1093/bioinformatics/btr330.

Darlington, Jr., P.J., 1957. Zoogeography: The Geographical Distribution of Animals. Jhon Wiley & Sons Inc.

Darriba, D., Taboada, G.L., Doallo, R., Posada, D., 2012. jModelTest 2: more models, new heuristics and parallel computing. Nat. Methods 9, 772. https://doi.org/10.1038/nmeth.2109.

DaSilva, M.B., Pinto-da-Rocha, R., DeSouza, A.M., 2015. A protocol for the delimitation of areas of endemism and the historical regionalization of the Brazilian Atlantic Rain Forest using harvestmen distribution data. Cladistics 31, 692–705. https://doi.org/10.1111/cla.12121.

de Oliveira Miranda, N.E., Maciel, N.M., Lima-Ribeiro, M.S., Colli, G.R., Haddad, C.F.B., Collevatti, R.G., 2019. Diversification of the widespread neotropical frog *Physalaemus cuvieri* in response to Neogene-Quaternary geological events and climate dynamics. Mol. Phylogenet. Evol. 132, 67–80. https://doi.org/10.1016/j.ympev.2018.11.003.

Delhey, K., 2017. Gloger's rule. Curr. Biol. 27, R689–R691. https://doi.org/10.1016/j.cub.2017.04.031.

Dickinson, E.C., Christidis, L., 2014. The Howard and Moore Complete Checklist of the Birds of the World. 4th ed., Vol. 2 Passerines.

Dinerstein, E., Olson, D., Joshi, A., Vynne, C., Burgess, N.D., Wikramanayake, E., Hahn, N., Palminteri, S., Hedao, P., Noss, R., Hansen, M., Locke, H., Ellis, E.C., Jones, B., Barber, C.V., Hayes, R., Kormos, C., Martin, V., Crist, E., Sechrest, W., Price, L., Baillie, J.E.M., Weeden, D., Suckling, K., Davis, C., Sizer, N., Moore, R., Thau, D., Birch, T., Potapov, P., Turubanova, S., Tyukavina, A., de Souza, N., Pintea, L., Brito, J.C., Llewellyn, O.A., Miller, A.G., Patzelt, A., Ghazanfar, S.A., Timberlake, J., Klöser, H., Shennan-Farpón, Y., Kindt, R., Lillesø, J.-P.B., van Breugel, P., Graudal, L., Voge, M., Al-Shammari, K.F., Saleem, M., 2017. An ecoregion-based approach to protecting half the terrestrial realm. Bioscience 67, 534–545. https://doi.org/10.1093/biosci/bix014.

Drummond, A.J., Suchard, M.A., Xie, D., Rambaut, A., 2012. Bayesian phylogenetics with BEAUti and the BEAST 1.7. Mol. Biol. Evol. 29, 1969–1973. https://doi.org/10.1093/molbev/mss075.

Faircloth, B.C., 2016. PHYLUCE is a software package for the analysis of conserved genomic loci. Bioinformatics 32, 786–788. https://doi.org/10.1093/bioinformatics/btv646.

Faircloth, B.C., 2013. Illumiprocessor: a trimmomatic wrapper for parallel adapter and quality trimming.

Faircloth, B.C., Mccormack, J.E., Crawford, N.G., Harvey, M.G., Brumfield, R.T., Glenn, T.C., 2012. Ultraconserved elements anchor thousands of genetic markers spanning multiple evolutionary timescales. Syst. Biol. 61, 717–726. https://doi.org/10.1093/sysbio/sys004.

Fiaschi, P., Pirani, J.R., 2009. Review of plant biogeographic studies in Brazil. J. Syst. Evol. 47, 477–496. https://doi.org/10.1111/j.1759-6831.2009.00046.x.

Florentín, J.E., Arana, M.D., Prado, D.E., Morrone, J.J., Salas, R.M., 2018. Diversification of *Galianthe* species (Rubiaceae) in the Neotropical seasonally dry forests: a case study of a mainly subshrubby genus. Plant Ecol. Evol. 151, 161–174. https://doi.org/10.5091/plecevo.2018.1419.

Frichot, E., François, O., 2015. LEA: An R package for landscape and ecological association studies. Methods Ecol. Evol. 6, 925–929. https://doi.org/10.1111/2041-210X.12382.

Frichot, E., Mathieu, F., Trouillon, T., Bouchard, G., François, O., 2014. Fast and efficient estimation of individual ancestry coefficients. Genetics 196, 973–983. https://doi.org/10.1534/genetics.113.160572.

García-Vázquez, D., Bilton, D.T., Foster, G.N., Ribera, I., 2017. Pleistocene range shifts, refugia and the origin of widespread species in Western Palaearctic water beetles. Mol. Phylogenet. Evol. 114, 122–136. https://doi.org/10.1016/j.ympev.2017.06.007.

Grabherr, M.G., Haas, B.J., Yassour, M., Levin, J.Z., Thompson, D.A., Amit, I., Adiconis, X., Fan, L., Raychowdhury, R., Zeng, Q., Chen, Z., Mauceli, E., Hacohen, N., Gnirke, A., Rhind, N., di Palma, F., Birren, B.W., Nusbaum, C., Lindblad-Toh, K., Friedman, N., Regev, A., 2011. Full-length transcriptome assembly from RNA-Seq data without a reference genome. Nat. Biotechnol. 29, 644–652. https://doi.org/10.1038/nbt.1883.

Graham, A., 2009. The Andes: a geological overview from a biological perspective. Ann. Missouri Bot. Gard. 96, 371–385. https://doi.org/10.3417/2007146.

Graves, G.R., 1991. Bergmann's rule near the equator: latitudinal clines in body size of an Andean passerine bird. Proc. Natl. Acad. Sci. 88, 2322–2325. https://doi.org/10.1073/pnas.88.6.2322.

Haffer, J., 1997. Alternative models of vertebrate speciation in Amazonia: an overview. Biodivers. Conserv. 6, 451–476.

Haffer, J., 1969. Speciation in Amazonian forest birds. Sci. New Ser. 165, 131–137.

Halffter, G., 1992. La Diversidad Biológica De Iberoamérica I. Instituto De Ecología, A.C. Secretaria De Desarrollo Social.

Harvey, M.G., Smith, B.T., Glenn, T.C., Faircloth, B.C., Brumfield, R.T., 2016. Sequence

capture versus restriction site associated DNA sequencing for shallow systematics. Syst. Biol. 65, 910–924. https://doi.org/10.1093/sysbio/syw036.
Hernández-Romero, P.C., Gutiérrez-Rodríguez, C., Valdespino, C., Prieto-Torres, D.A., 2017. The Role of Geographical and Ecological Factors on Population Divergence of the Neotropical otter *Lontra longicaudis* (Carnivora, Mustelidae). Evol. Biol. 45, 37–55. https://doi.org/10.1007/s11692-017-9428-5.
Herzog, S.K., Kattan, G.H., 2011. Patterns of Diversity and Endemism in the Birds of the Tropical Andes. In: Herzog, S K, Martínez, R., Jørgensen, P.M., Tiessen(Eds.), H. (Eds.), Climate Change and Biodiversity in the Tropical Andes. Inter-American Institute for Global Change Research (IAI) and Scientific Committee on Problems of the Environment (SCOPE, Paris, pp. 245–259.
Herzog, S.K., Martínez, R., Jørgensen, P.M., Tiessen, H., 2011. Climate Change and Biodiversity in the Tropical Andes. IAI.
Hooghiemstra, H., der Hammen, T. Van, Cleef, A., 2002. Evolution of forests in the northern Andes and Amazonian lowlands during the Tertiary and Quaternary in Ecology of neotropical rain forests. In: Guariguata, M.R., Kattan, G.H. (Eds.), Editorial Cartago, Libro Universitario Regional (EULAC-GTZ), CR.
Hoorn, C., Wesselingh, F.P., ter Steege, H., Bermudez, M.A., Mora, A., Sevink, J., Sanmartín, I., Sanchez-Meseguer, A., Anderson, C.L., Figueiredo, J.P., Jaramillo, C., Riff, D., Negri, F.R., Hooghiemstra, H., Lundberg, J., Stadler, T., Särkinen, T., Antonelli, A., 2010. Amazonia Through Time: Andean Uplift. Climate Change, Landscape Evolution, and Biodiversity. Science (80-.). 330,, 927–931. https://doi.org/10.1126/science.1194585.
Hosner, P.A., Braun, E.L., Kimball, R.T., 2016. Rapid and recent diversification of curassows, guans, and chachalacas (Galliformes: Cracidae) out of Mesoamerica: Phylogeny inferred from mitochondrial, intron, and ultraconserved element sequences. Mol. Phylogenet. Evol. 102, 320–330. https://doi.org/10.1016/j.ympev.2016.06.006.
Huang, H., Knowles, L., 2016. Unforeseen consequences of excluding missing data from next-generation sequences: Simulation study of rad sequences. Syst. Biol. 65, 357–365. https://doi.org/10.1093/sysbio/syu046.
Hurvich, C.M., Tsai, C.-L., 1989. Regression and time series model selection in small samples. Biometrika 76, 297–307. https://doi.org/10.1093/biomet/76.2.297.
Irmler, U., 2009. New species and records of the genus *Lispinus* with a key to the species from Peru (Coleoptera: Staphylinidae: Osoriinae). Zootaxa 2263, 42–58.
Isler, M.L., Isler, P.R., Brumfield, R.T., Zink, R.M., 2005. Clinal variation in vocalizations of an antbird (Thamnophilidae) and implications for defining species limits. Auk 122, 433–444. https://doi.org/10.1642/0004-8038(2005)122[0433:CVIVOA]2.0.CO;2.
Jombart, T., 2008. *adegenet*: a R package for the multivariate analysis of genetic markers. Bioinformatics 24, 1403–1405. https://doi.org/10.1093/bioinformatics/btn129.
Jombart, T., Devillard, S., Balloux, F., 2010. Discriminant analysis of principal components: a new method for the analysis of genetically structured populations. BMC Genet. 11, 94. https://doi.org/10.1186/1471-2156-11-94.
Kamm, J., Terhorst, J., Durbin, R., Song, Y., 2019. Efficiently Inferring the Demographic History of Many Populations With Allele Count Data. Journal of the American Statistical Association 1–16. https://doi.org/10.1080/01621459.2019.1635482.
Kamvar, Z.N., Brooks, J.C., Grünwald, N.J., 2015. Novel R tools for analysis of genome-wide population genetic data with emphasis on clonality. Front. Genet. 6, 208. https://doi.org/10.3389/fgene.2015.00208.
Kamvar, Z.N., Tabima, J.F., Grünwald, N.J., 2014. *Poppr*: an R package for genetic analysis of populations with clonal, partially clonal, and/or sexual reproduction. PeerJ 2, e281. https://doi.org/10.7717/peerj.281.
Katoh, K., Standley, D.M., 2013. MAFFT multiple sequence alignment software version 7: improvements in performance and usability. Mol. Biol. Evol. 30, 772–780. https://doi.org/10.1093/molbev/mst010.
Kearse, M., Moir, R., Wilson, A., Stones-Havas, S., Cheung, M., Sturrock, S., Buxton, S., Cooper, A., Markowitz, S., Duran, C., Thierer, T., Ashton, B., Meintjes, P., Drummond, A., 2012. Geneious Basic: An integrated and extendable desktop software platform for the organization and analysis of sequence data. Bioinformatics 28, 1647–1649. https://doi.org/10.1093/bioinformatics/bts199.
Knapp, S., 2002. Assessing patterns of plant endemism in neotropical uplands. Bot. Rev. 68, 22–37.
Lamichhaney, S., Card, D.C., Grayson, P., Tonini, J.F.R., Bravo, G.A., Npflin, K., Termignoni-Garcia, F., Torres, C., Burbrink, F., Clarke, J.A., Sackton, T.B., Edwards, S. V, 2019. Integrating natural history collections and comparative genomics to study the genetic architecture of convergent evolution. Philos. Trans. R. Soc. B Biol. Sci. 374, 20180248. https://doi.org/10.1098/rstb.2018.0248.
Kopuchian, C., Campagna, L., Lijtmaer, D.A., Cabanne, G.S., García, N.C., Lavinia, P.D., Tubaro, P.L., Lovette, I., Di Giacomo, A.S., 2020. A test of the riverine barrier hypothesis in the largest subtropical river basin in the Neotropics. Molecular Ecology mec.15384. https://doi.org/10.1111/mec.15384.
Leal, B.S.S., Medeiros, L.R., Peres, E.A., Sobral-Souza, T., Palma-Silva, C., Romero, G.Q., Carareto, C.M.A., 2018. Insights into the evolutionary dynamics of Neotropical biomes from the phylogeography and paleodistribution modeling of *Bromelia balansae*. Am. J. Bot. 105, 1725–1734. https://doi.org/10.1002/ajb2.1167.
Leigh, J.W., Bryant, D., 2015. popart: full-feature software for haplotype network construction. Methods Ecol. Evol. 6, 1110–1116. https://doi.org/10.1111/2041-210X.12410.
Li, H., 2013. Aligning sequence reads, clone sequences and assembly contigs with BWA-MEM. arXiv arXiv:1303.3997v2 [q-bio.GN].
Li, H., Durbin, R., 2009. Fast and accurate short read alignment with Burrows-Wheeler transform. Bioinformatics 25, 1754–1760. https://doi.org/10.1093/bioinformatics/btp324.
Li, H., Handsaker, B., Wysoker, A., Fennell, T., Ruan, J., Homer, N., Marth, G., Abecasis, G., Durbin, R., Subgroup, 1000 Genome Project Data Processing, 2009. The Sequence Alignment/Map format and SAMtools. Bioinformatics 25, 2078–2079. https://doi.org/10.1093/bioinformatics/btp352.
Linares-Palomino, R., Oliveira-Filho, A.T., Pennington, R.T., 2011. Neotropical Seasonally Dry Forests: Diversity, Endemism, and Biogeography of Woody Plants. In: Seasonally Dry Tropical Forests. Island Press/Center for Resource Economics, Washington, DC, pp. 3–21. https://doi.org/10.5822/978-1-61091-021-7_1.
Luebert, F., Weigend, M., 2014. Phylogenetic insights into Andean plant diversification. Front. Genet. 2, 27. https://doi.org/10.3389/fevo.2014.00027.
Maldonado-Coelho, M., 2012. Climatic oscillations shape the phylogeographical structure of Atlantic Forest fire-eye antbirds (Aves: Thamnophilidae). Biol. J. Linn. Soc. 105, 900–924. https://doi.org/10.1111/j.1095-8312.2011.01823.x.
Maldonado-Coelho, M., Blake, J.G., Silveira, L.F., Batalha-filho, H., Ricklefs, R.E., 2013. Rivers, refuges and population divergence of fire-eye antbirds (*Pyriglena*) in the Amazon Basin. J. Evol. Biol. 26, 1090–1107. https://doi.org/10.1111/jeb.12123.
Marcondes S., Rafael, Stryjewski F., K., Brumfield T., Robb, 2020. Extraordinary plumage color variation and Gloger's rule in *Thamnophilus caerulescens* (Passeriformes, Thamnophilidae). The Auk In press.
McKenna, A., Hanna, M., Banks, E., Sivachenko, A., Cibulskis, K., Kernytsky, A., Garimella, K., Altshuler, D., Gabriel, S., Daly, M., DePristo, M.A., 2010. The Genome analysis toolkit: A MapReduce framework for analyzing next-generation DNA sequencing data. Genome Res. 20, 1297–1303. https://doi.org/10.1101/gr.107524.110.
Melo Santos, A.M., Cavalcanti, D.R., da Silva, J.M.C., Tabarelli, M., 2007. Biogeographical relationships among tropical forests in north-eastern Brazil. J. Biogeogr. 34, 437–446. https://doi.org/10.1111/j.1365-2699.2006.01604.x.
Miller, M.J., Bermingham, E., Klicka, J., Escalante, P., Winker, K., 2010b. Neotropical birds show a humped distribution of within-population genetic diversity along a latitudinal transect. Ecol. Lett. 13, 576–586. https://doi.org/10.1111/j.1461-0248.2010.01454.x.
Mittermeier, R.A., Myers, N., Thomsen, J.B., da Fonseca, G.A.B., Olivieri, S., 1998. Biodiversity hotspots and major tropical wilderness areas: approaches to setting conservation priorities. Conserv. Biol. 12, 516–520. https://doi.org/10.1046/j.1523-1739.1998.012003516.x.
Mogni, V.Y., Oakley, L.J., Prado, D.E., 2015. The distribution of woody legumes in neotropical dry forests: the Pleistocene Arc Theory 20 years on* Edinburgh J. Bot. 72, 35–60. https://doi.org/10.1017/S0960428614000298.
Miller, M. A., Pfeiffer, W., Schwartz, T., 2010. Creating the CIPRES Science Gateway for Inference of Large Phylogenetic Trees. In: Proceedings of the Gateway Computing Environments Workshop (GCE). New Orleans, LA, pp. 1–8.
Mooney, H.A., Bullock, S.H., Medina, E., 1995. Introduction. In: Bullock, S.H., Mooney, H. A., Medina, ErnestoEditors (Eds.), Seasonally Dry Tropical Forests. Cambridge University Press, pp. 1–8. https://doi.org/10.1017/CBO9780511753398.001.
Morrone, J.J., 2014. Biogeographical regionalisation of the Neotropical region. Zootaxa 3782, 1–110. https://doi.org/10.11646/zootaxa.3782.1.1.
Myers, N., Mittermeier, R.A., Mittermeier, C.G., da Fonseca, G.A.B., Kent, J., 2000. Biodiversity hotspots for conservation priorities. Nature 403, 853–858.
Nabholz, B., Lanfear, R., Fuchs, J., 2016. Body mass-corrected molecular rate for bird mitochondrial DNA. Mol. Ecol. 25, 4438–4449. https://doi.org/10.1111/mec.13780.
Nace, T.E., Baker, P.A., Dwyer, G.S., Silva, C.G., Rigsby, C.A., Burns, S.J., Giosan, L., Otto-Bliesner, B., Liu, Z., Zhu, J., 2014. The role of North Brazil Current transport in the paleoclimate of the Brazilian Nordeste margin and paleoceanography of the western tropical Atlantic during the late Quaternary. Palaeogeogr. Palaeoclimatol. Palaeoecol. 415, 3–13. https://doi.org/10.1016/j.palaeo.2014.05.030.
Nadachowska-Brzyska, K., Li, C., Smeds, L., Zhang, G., Ellegren, H., 2015. Temporal dynamics of avian populations during pleistocene revealed by whole-genome sequences. Curr. Biol. 25, 1375–1380. https://doi.org/10.1016/j.cub.2015.03.047.
Naka, L.N., Brumfield, R.T., 2018. The dual role of Amazonian rivers in the generation and maintenance of avian diversity. Sci. Adv. 4. https://doi.org/10.1126/sciadv.aar8575.
Olson, D.M., Dinerstein, E., Wikramanayake, E.D., Burgess, N.D., Powell, G.V.N., Underwood, E.C., D'Amico, J.A., Itoua, I., Strand, H.E., Morrison, J.C., Loucks, C.J., Allnutt, T.F., Ricketts, T.H., Kura, Y., Lamoreux, J.F., Wettengel, W.W., Hedao, P., Kassem, K.R., 2001. Terrestrial Ecoregions of the World: A New Map of Life on Earth. Bioscience 52, 933–938.
Paradis, E., 2010. pegas: an R package for population genetics with an integrated–modular approach. Bioinformatics 26, 419. https://doi.org/10.1093/bioinformatics/btp696.
Paradis, E., Claude, J., Strimmer, K., 2004. APE: analyses of phylogenetics and evolution in R language. Bioinformatics 20, 289–290. https://doi.org/10.1093/bioinformatics/btg412.
Pérez-Escobar, O.A., Chomicki, G., Condamine, F.L., Karremans, A.P., Bogarín, D., Matzke, N.J., Silvestro, D., Antonelli, A., 2017. Recent origin and rapid speciation of Neotropical orchids in the world's richest plant biodiversity hotspot. New Phytol. 215, 891–905. https://doi.org/10.1111/nph.14629.
Polato, N.R., Gill, B.A., Shah, A.A., Gray, M.M., Casner, K.L., Barthelet, A., Messer, P.W., Simmons, M.P., Guayasamin, J.M., Encalada, A.C., Kondratieff, B.C., Flecker, A.S., Thomas, S.A., Ghalambor, C.K., Poff, N.L., Funk, W.C., Zamudio, K.R., 2018. Narrow thermal tolerance and low dispersal drive higher speciation in tropical mountains. Proc. Natl. Acad. Sci. 115, 12471–12476. https://doi.org/10.1073/pnas.1809326115.
Prado, D.E., Gibbs, P.E., 1993. Patterns of species distributions in the dry seasonal forests of South America. Ann. Missouri Bot. Gard. 80, 902–927.
Prance, G.T., 1982. Biological Diversification in the Tropics. Columbia University Press.
Prates, I., Melo-Sampaio, P.R., de Oliveira Drummond, L., Jr., M.T., Rodrigues, M.T., Carnaval, A.C., 2017. Biogeographic links between southern Atlantic Forest and western South America: rediscovery, re-description, and phylogenetic relationships of two rare montane anole lizards from Brazil. Mol. Phylogenet. Evol. 113, 49–58.

https://doi.org/https://doi.org/10.1016/j.ympev.2017.05.009.
Premoli, A.C., 2003. Isozyme polymorphisms provide evidence of clinal variation with elevation in *Nothofagus pumilio*. J. Hered. 94, 218–226. https://doi.org/10.1093/jhered/esg052.
Prieto-Torres, D.A., Cuervo, A.M., Bonaccorso, E., 2018. On geographic barriers and Pleistocene glaciations: Tracing the diversification of the Russet-crowned Warbler *(Myiothlypis coronata*) along the Andes. PLoS One 13, 1–15. https://doi.org/10.1371/journal.pone.0191598.
Pulido-Santacruz, P., Bornschein, M.R., Belmonte-Lopes, R., Bonatto, S.L., 2016. Multiple evolutionary units and demographic stability during the last glacial maximum in the *Scytalopus speluncae* complex (Aves: Rhinocryptidae). Mol. Phylogenet. Evol. 102, 86–96. https://doi.org/10.1016/j.ympev.2016.05.027.
Quijada-Mascarenãs, J.A., Ferguson, J.E., Pook, C.E., Salomão, M.D.G., Thorpe, R.S., Wüster, W., 2007. Phylogeographic patterns of trans-Amazonian vicariants and Amazonian biogeography: the Neotropical rattlesnake (*Crotalus durissus* complex) as an example. J. Biogeogr. 34, 1296–1312. https://doi.org/10.1111/j.1365-2699.2007.01707.x.
Rambaut, A., 2009. FigTree version 1.3.1.
Rambaut, A., Drummond, A.J., Xie, D., Baele, G., Suchard, M.A., 2018. Posterior summarization in bayesian phylogenetics using tracer 1.7. Syst. Biol. 67, 901–904. https://doi.org/10.1093/sysbio/syy032.
Ramos, E.K.S., de Magalhes, R.F., Marques, N.C.S., Bata, D., Garcia, P.C.A., Santos, F.R., 2018. Cryptic diversity in Brazilian endemic monkey frogs (Hylidae, Phyllomedusinae, *Pithecopus*) revealed by multispecies coalescent and integrative approaches. Mol. Phylogenet. Evol. 132, 105–116. https://doi.org/10.1016/j.ympev.2018.11.022.
Remsen, J.V., Rocha, O., Schmitt, C.G., Schmitt, D.C., 1991. Zoogeography and geographic variation of *Platyrinchus mystaceus* in Bolivia and Peru, and the Circum-amazonian distribution pattern. Ornitol. Neotrop. 2, 77–83.
von Rensch, B., 1929. Das Prinzip geographischer Rassenkreise und das Problem der Artbildung. Nature 124, 753–754. https://doi.org/10.1038/124753a0.
Richardson, J.E., Pennington, R.T., Pennington, T.D., Hollingsworth, P.M., 2001. Rapid diversification of a species-rich genus of neotropical rain forest trees. Science (80-.) 293, 2242–2245. https://doi.org/10.1126/science.1061421.
Rozas, J., Ferrer-Mata, A., Sanchez-DelBarrio, J.C., Guirao-Rico, S., Librado, P., Ramos-Onsins, S.E., Sanchez-Gracia, A., 2017. DnaSP 6: DNA sequence polymorphism analysis of large data sets. Mol. Biol. Evol. 34, 3299–3302. https://doi.org/10.1093/molbev/msx248.
Sánchez-González, L.A., Morrone, J.J., Navarro-Sigüenza, A.G., 2008. Distributional patterns of the Neotropical humid montane forest avifaunas. Biol. J. Linn. Soc. 94, 175–194. https://doi.org/10.1111/j.1095-8312.2008.00979.x.
Savit, A.Z., Bates, J.M., 2015. Right around the Amazon: the origin of the circum-Amazonian distribution in *Tangara cayana*. Folia Zool. 64, 273–283.
Seeholzer, G.F., Brumfield, R.T., 2018. Isolation by distance, not incipient ecological speciation, explains genetic differentiation in an Andean songbird (Aves: Furnariidae: *Cranioleuca antisiensis*, Line-cheeked Spinetail) despite near threefold body size change across an environmenta. Mol. Ecol. 27, 279–296. https://doi.org/10.1111/mec.14429.
Sick, H., 1967. Rios e enchentes na Amazonia como obstáculo para a avifauna. Atas Simp. Sobre a Biota Amaz. 5, 495–520.
Silva, J.M.C., de Sousa, M.C., Castelletti, C.H.M., 2004. Areas of endemism for passerine birds in the Atlantic forest, South America. Glob. Ecol. Biogeogr. 13, 85–92. https://doi.org/10.1111/j.1466-882X.2004.00077.x.
Silveira, L., Olmos, F., J. Long, A., 2003. Birds in Atlantic Forest fragments in north-east Brazil. Cotinga 20, 32–46.
Smith, B.T., McCormack, J.E., Cuervo, A.M., Hickerson, M.J., Aleixo, A., Cadena, C.D., Pérez-Emán, J., Burney, C.W., Xie, X., Harvey, M.G., Faircloth, B.C., Glenn, T.C., Derryberry, E.P., Prejean, J., Fields, S., Brumfield, R.T., 2014. The drivers of tropical speciation. Nature 515, 406–409. https://doi.org/10.1038/nature13687.
Stotz, D.F., Fitzpatrick, J.W., Parker, T.A.I.I.I., Moskovits, D.K., 1996. Neotropical birds: Ecology and Conservation. University of Chicago Press.
Tabarelli, M., Aguiar, A.V., Ribeiro, M.C., Metzger, J.P., Peres, C.A., 2010. Prospects for biodiversity conservation in the Atlantic Forest: Lessons from aging human-modified landscapes. Biol. Conserv. 143, 2328–2340. https://doi.org/10.1016/j.biocon.2010.02.005.
Tello, J.G., Raposo, M., Bates, J.M., Bravo, G.A., Cadena, C.D., Maldonado-Coelho, M., 2014. Reassessment of the systematics of the widespread Neotropical genus *Cercomacra* (Aves: Thamnophilidae). Zool. J. Linn. Soc. 170, 546–565. https://doi.org/10.1111/zoj.12116.
Thom, G., Aleixo, A., 2015. Cryptic speciation in the white-shouldered antshrike (*Thamnophilus aethiops*, Aves – Thamnophilidae): The tale of a transcontinental radiation across rivers in lowland Amazonia and the northeastern Atlantic Forest. Mol. Phylogenet. Evol. 82, 95–110. https://doi.org/10.1016/j.ympev.2014.09.023.
Thom, G., Amaral, F.R. Do, Hickerson, M.J., Aleixo, A., Araujo-Silva, L.E., Ribas, C.C., Choueri, E., Miyaki, C.Y., 2018. Phenotypic and genetic structure support gene flow generating gene tree discordances in an Amazonian floodplain endemic species. Syst. Biol. 67, 700–718. https://doi.org/10.1093/sysbio/syy004.
Thomaz, A.T., Malabarba, L.R., Bonatto, S.L., Knowles, L.L., 2015. Testing the effect of palaeodrainages versus habitat stability on genetic divergence in riverine systems: study of a Neotropical fish of the Brazilian coastal Atlantic Forest. J. Biogeogr. 42, 2389–2401. https://doi.org/10.1111/jbi.12597.
Thomé, M.T.C., Zamudio, K.R., Giovanelli, J.G.R., Haddad, C.F.B., Jr., F.A.B., Alexandrino, J., 2010. Phylogeography of endemic toads and post-Pliocene persistence of the Brazilian Atlantic Forest. Mol. Phylogenet. Evol. 55, 1018–1031. https://doi.org/https://doi.org/10.1016/j.ympev.2010.02.003.
Trujillo-Arias, N., Calderón, L., Santos, F.R., Miyaki, C.Y., Aleixo, A., Witt, C.C., Tubaro, P.L., Cabanne, G.S., 2018. Forest corridors between the central Andes and the southern Atlantic Forest enabled dispersal and peripatric diversification without niche divergence in a passerine. Mol. Phylogenet. Evol. 128, 221–232. https://doi.org/10.1016/j.ympev.2018.08.005.
Trujillo-Arias, N., Dantas, G., Arbeláez-Cortés, E., Naoki, K., Gómez, M.I., Santos, F.R., Miyaki, C.Y., Aleixo, A., Tubaro, P.L., Cabanne, G.S., 2017. The niche and phylogeography of a passerine reveal the history of biological diversification between the Andean and the Atlantic forests. Mol. Phylogenet. Evol. 112, 107–121. https://doi.org/10.1016/j.ympev.2017.03.025.
Van Doren, B.M., Freeman, B.G., Aristizabal, N., Alvarez-R, M., Pérez-Emán, J., Cuervo, A.M., Bravo, G.A., 2018. Species limits in the Rusty-breasted Antpitta (*Grallaricula ferrugineipectus*) complex. Wilson J. Ornithol. 130, 152–167. https://doi.org/10.1676/16-126.1.
Vanzolini, P.E., Williams, E.E., 1981. The Vanishing Refuge: A mechanism for ecogeographic speciation. Pap. Avulsos Zool. 34, 251–255.
Vanzolini, P.E., Williams, E.E., 1970. South American anoles: The geographic differentiation and evolution of the anolis *Chrysolepis* species group (Sauria, Iguanidae). In: Arquivos de. zoologia. Museu de Zoologia.
Wallace, A.R., 1854. On the Monkeys of the Amazon. Ann. Mag. Nat. Hist. 14, 451–454. https://doi.org/10.1080/037454809494374.
Wang, X., Edwards, R.L., Auler, A.S., Cheng, H., Kong, X., Wang, Y., Cruz, F.W., Dorale, J.A., Chiang, H.-W., 2017. Hydroclimate changes across the Amazon lowlands over the past 45,000 years. Nature 541, 204–207. https://doi.org/10.1038/nature20787.
Werneck, F.P., Costa, G.C., Colli, G.R., Prado, D.E., Sites Jr, J.W., 2011. Revisiting the historical distribution of Seasonally Dry Tropical Forests: new insights based on palaeodistribution modelling and palynological evidence. Glob. Ecol. Biogeogr. 20, 272–288. https://doi.org/10.1111/j.1466-8238.2010.00596.x.
Werneck, F.P., Gamble, T., Colli, G.R., Rodrigues, M.T., Sites Jr, J.W., 2012. Deep diversification and long-term persistence in the south american “Dry Diagonal”: Integrating continent-wide phylogeography and distribution modeling of geckos. Evolution (N. Y) 66, 3014–3034. https://doi.org/10.1111/j.1558-5646.2012.01682.x.
Xi, Z., Liu, L., Davis, C.C., 2015. Genes with minimal phylogenetic information are problematic for coalescent analyses when gene tree estimation is biased. Mol. Phylogenet. Evol. 92, 63–71. https://doi.org/10.1016/j.ympev.2015.06.009.
Zimmer, K.J., and Isler, M.L. (2003). Variable Antshrike (*Thamnophilus caerulescens*). Pp. 561-562 In: del Hoyo, J., Elliott, A., and Christie, D. A. eds.(2003). *Handbook of the Birds of the World.* Vol. 8. Broadbills of Tapaculos. Lynx Edicions, Barcelona. ISBN 84-87334-50-4.

Update

Molecular Phylogenetics and Evolution

Volume 150, Issue , September 2020, Page

DOI: https://doi.org/10.1016/j.ympev.2020.106890

Molecular Phylogenetics and Evolution 150 (2020) 106890

Contents lists available at ScienceDirect

Molecular Phylogenetics and Evolution

journal homepage: www.elsevier.com/locate/ympev

Corrigendum

Corrigendum to "Phylogeography of the Variable Antshrike (*Thamnophilus caerulescens*), a South American passerine distributed along multiple environmental gradients" [Mol. Phylogenet. Evol. 148 (2020) 106810]

Sergio D. Bolívar-Leguizamón[a,*], Luís F. Silveira[a], Elizabeth P. Derryberry[b], Robb T. Brumfield[c,d], Gustavo A. Bravo[a,e,f]

[a] Museu de Zoologia da Universidade de São Paulo, 04263-000 Ipiranga, São Paulo, SP, Brazil
[b] Department of Ecology and Evolutionary Biology, University of Tennessee, Knoxville, TN 37996, USA
[c] Department of Biological Sciences, Louisiana State University, Baton Rouge, LA 70803, USA
[d] Museum of Natural Science, Louisiana State University, Baton Rouge, LA 70803, USA
[e] Department of Organismic and Evolutionary Biology, Harvard University, Cambridge, MA 02138, USA
[f] Museum of Comparative Zoology, Harvard University, Cambridge, MA 02138, USA

The authors regret:

(a) The information of Table 2 has incorrect values in column 6. The following table has the correct values.

(b) Also, there is a minor typo in the section 'Data accessibility', in the word: 'alignmentsare'. The correct words are: 'alignments are'.

The authors would like to apologize for any inconvenience caused.

Table 2
Information theory statistics and ranking of the 16 demographic models evaluated with momi2 using the incomplete matrix (2036 SNPs). For a complete list of parameter values see Table S9. The most informative models included parameters related to divergence and migration events only.

Rank	Type of model	Model number	Log-lik	Number of parameters	ΔAIC	ω_i
1	**Migrations & divergence**	**7**	**−7290.17**	**13**	0.00	**1.00**
2	Migrations & divergence	6	−7299.86	9	42.71	5.32E−10
3	Migrations & divergence	4	−7323.52	9	90.03	2.83E−20
4	Migrations & divergence	5	−7345.25	9	133.47	1.04E−29
5	Migrations & divergence	2	−7383.25	4	201.48	1.77E−44
6	Migrations & divergence	3	−7386.64	5	208.27	5.96E−46
7	Migrations, divergence & expansion	10	−7388.48	16	233.95	1.58E−51
8	Migrations, divergence, expansion & bottlenecks	13	−7394.48	16	245.94	3.93E−54
9	Migrations, divergence & expansion	11	−7394.50	16	245.98	3.85E−54
10	Migrations & divergence	1	−7481.58	2	392.14	7.06E−86
11	Migrations, divergence & expansion	12	−7522.21	11	491.41	1.96E−107
12	Migrations, divergence & expansion	9	−7528.52	11	504.03	3.57E−110
13	Migrations, divergence & expansion	8	−7574.60	11	596.18	3.48E−130
14	Migrations, divergence, expansion & bottlenecks	15	−7621.89	13	706.75	3.40E−154
15	Migrations, divergence, expansion & bottlenecks	16	−7724.95	19	896.89	1.75E−195
16	Migrations, divergence, expansion & bottlenecks	14	−7807.85	11	1062.69	1.74E−231

DOI of original article: https://doi.org/10.1016/j.ympev.2020.106810
* Corresponding author.
E-mail addresses: bolivaruis@gmail.com, eldarin2003@yahoo.com (S.D. Bolívar-Leguizamón).

https://doi.org/10.1016/j.ympev.2020.106890

Available online 26 June 2020